# Reviews

## The nature and dynamics of nonlinear excitations in conducting polymers. Polyaniline

*V. I. Krinichnyi*

*Institute of Problems of Chemical Physics, Russian Academy of Sciences, 142432 Chernogolovka, Moscow Region, Russian Federation. Fax: +7 (096) 515 3588. E-mail: kivi@cat.icp.ac.ru*

The advantages of using the multifrequency (3-cm, 8-mm, and 2-mm) EPR method in combination with the modified method of spin label and spin probes and the methods of steady-state microwave saturation and microwave saturation transfer of spin packets in studies of the spin and electrodynamic properties of polyaniline are outlined. The methods of determining the composition of localized and delocalized paramagnetic centers and calculating their main parameters from total ESR spectra are described. Original results of investigations of polyaniline modified with sulfuric, hydrochloric, camphorsulfonic, and 2-acrylamido-2-methyl-1-propanesulfonic acids are reported. The dependences of the nature, electronic relaxation, dynamics of paramagnetic centers, and the charge-transfer mechanism on the method of synthesis, the structure of the acid molecule, and the polyaniline oxidation level are shown.

**Key words:** polyaniline, conducting polymers, EPR, spin, conducting mechanism, polaron.

The class of organic conductors comprises molecular crystals based on charge-transfer complexes and radical-ionic salts, fullerenes, platinum cyanide complexes, phthalocyanine dyes, metal-containing polymers,[1—5] and other compounds. These substances, especially a new class of electronic materials, namely, conducting organic polymers (COP) possessing a wide variety of electronic and magnetic properties,[6—12] are of interest from the viewpoint of studying fundamental problems of charge transfer. Investigation of COP is due to the development of basically new scientific concepts of electronic processes occurring in these substances and the vast potentialities of using them in molecular electronics.[13—19]

These materials have a highly anisotropic quasi-one-dimensional (Q1D) π-conducting structure with delocalized charge carriers, which strongly differentiates such systems from both conventional inorganic semiconductors (*e.g.*, silicon and selenium) and polymeric insulators (*e.g.*, polyethylene). Due to the chain structure of COP, a strong (specific of 1D-systems) interaction between the electron states occurs in these compounds, giving rise to conformational excitations, solitons, and polarons. Electronic properties of film-like or powder-like COP can be controlled and reversibly changed by chemical (electrochemical) oxidation or reduction. Their specific conductivity measured with direct current ($\sigma_{dc}$) varies from ~$10^{-10}$—$10^{-8}$ S m$^{-1}$, which is characteristic of insulators, to ~$10^{3}$—$10^{7}$ S m$^{-1}$, which is typical of classical metals. The conductivity type of a COP is determined by the nature of the counterion introduced into the polymer. For instance, the $BF_4^-$, $ClO_4^-$, $AsF_5^-$, $I_3^-$, $FeCl_4^-$, and $MnO_4^-$ anions, *etc.*, induce a positive charge of the polymer chain, thus resulting in *p*-type

Translated from *Izvestiya Akademii Nauk. Seriya Khimicheskaya*, No. 2, pp. 205—230, February, 2000.

1066-5285/00/4902-0207 $25.00 

conductivity of the polymer. Doping of the polymer with $Li^+$, $K^+$, $Na^+$, and other alkali metal ions results in *n*-type conductivity.

In the classical inorganic 3D semiconductors, each atom is covalently bound to its environment, thus determining the lattice rigidity. Therefore, electrons and holes (vacancies) are dominating excitations in such a rigid system. A fundamentally different situation occurs in the case of COP. Because of the specific 1D structure, such systems are much more sensitive to structural distortion. Therefore, electrophysical properties of conducting polymers are usually considered in the framework of the band theory[20] or the soliton-polaron theory[21,22] based on the Peierls instability typical of Q1D systems.[23] Organic conducting polymers are characterized by the carbon π-electron system with a partly filled conduction band, which determines the most important electronic properties of these systems.

One of the most studied and simplest COP is polyacetylene (PAc), in which the charge is transferred by a soliton.[21,24] To explain the experimental dependences of the conductivity of lightly doped *trans*-polyacetylene (*trans*-PAc) on the temperature, pressure, and frequency, a model was proposed[25] of interchain hopping electron transport between isoenergetic levels of neutral and charged solitons. This model was successfully used for identification of the charge transfer mechanism in *trans*-PAc.[26] The increase in the doping level of the polymer changes this mechanism, so tunneling of the charge between neighboring highly conducting domains[27] in the framework of the Sheng[28] or Mott[29] models involving variable range hopping (VRH) of the charge carriers occurs in the polymer instead of isoenergetic electron hopping. The highest conductivity of oriented *trans*-PAc is ~$10^7$ S $m^{-1}$ at room temperature[30,31]; however, it is 1-2 orders of magnitude lower than the value predicted theoretically for metal-like clusters in the polymer.[32]

Electronic and magnetic properties of poly(*para*-phenylene) (PPP) and analogous COP are for the most part similar to those of *trans*-PAc.[6–12,33,34] The ground state of these COP is nondegenerate[21] and that is the reason why, unlike with PAc, no solitons can be formed in this case. However, it was reported[35,36] that the soliton-antisoliton pairs can also be stabilized in PPP as polarons and bipolarons. It was also hypothesized[37] that isoenergetic charge transfer can occur not only in *trans*-PAc, but also in other conducting polymers with soliton-like nonlinear excitations. In fact, experiments have shown[38] that the Kivelson mechanism[25] plays an important role in both *dc* and *ac* charge transfer (at a frequency of 25 GHz) in lightly doped PPP. Experimental studies have shown that, as in the case of *trans*-PAc, the charge transfer in doped PPP-like COP follows the Mott mechanism (see, *e.g.*, Refs. 38–44).

Among PPP-like COP, polyaniline (PAn) is the most stable and promising. Depending on the degree of oxidation or protonation, PAn can exist in the following forms[34]:

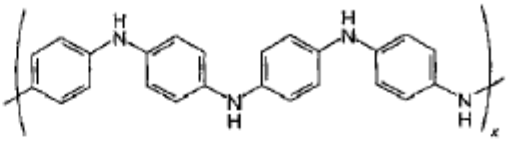

Leucoemeraldine (LE)

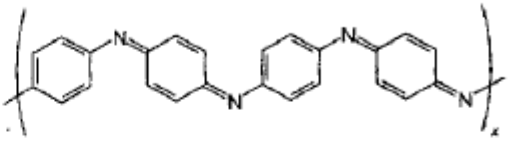

Pernigraniline (PN)

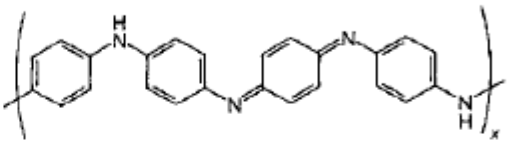

Emeraldine base (EB)

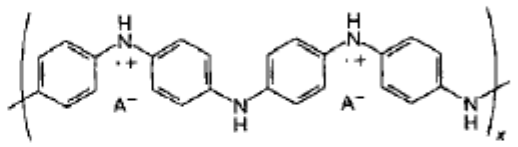

Emeraldine salt (ES(A))

In the last case, the symbol A denotes the anion of the acid used for the doping of PAn, *e.g.*, sulfate, chloride, camphorsulfonate (CS), or 2-acrylamido-2-methyl-1-propanesulfonate (AMPS) anions.

The lattice constants determined for the EB form of PAn are $a$ = 0.765, $b$ = 0.575, and $c$ = 1.020 nm.[45] Protonation of the EB or oxidation of the LE form of PAn results in an increase in the polymer conductivity by more than 10 orders of magnitude and in the appearance of the Pauli magnetic susceptibility typical of metals.[46,47] This indicates the formation of highly conducting fully protonated or oxidized clusters in the amorphous polymer. In this case the effective crystallinity of the polymer (*e.g.*, PAn · HCl) increases by ~50% owing to the formation of crystallites with a characteristic size of about 5 nm.[48] The lattice constants for the PAn · ES(A) form are $a$ = 0.430, $b$ = 0.590, and $c$ = 0.960 nm (for PAn · $H_2SO_4$)[49]; $a$ = 0.700, $b$ = 0.860, and $c$ = 1.040 nm (for PAn · HCl)[45]; and $a$ = 0.590, $b$ = 1.000, and $c$ = 0.720 nm (for PAn · CS).[50] The crystallinity and, hence, conducting properties of PAn are strongly dependent on the structure of the dopant introduced. As was shown by optical reflection (at 0.06–6.0 eV),[50,51] PAn · CS is a disordered Drude-like metal with free charge carriers delocalized over a partly filled conduction band. In the more disordered PAn · $H_2SO_4$, the

charge carriers are localized near the Fermi level, which is typical of a Fermi glass and results in increase in the crystallinity and in strengthening of metallic properties of the polymer in the series PAn · CS → PAn · $H_2SO_4$ → PAn · HCl at comparable doping levels. However, in some instances this conclusion is inconsistent with the results obtained by other authors in studies of PAn carried out by other methods.

It was shown theoretically and experimentally[52] that in PAn, as in other COP, the charge carriers are polarons moving along individual polymer chains. At low degree of oxidation, the hopping charge transfer between polarons and bipolarons dominates in PAn. As for other COP, the number of such charge carriers increases on further oxidation, while their energy levels merge to form a metal-like band structure, the so-called polaron lattice.[49,53]

Macroscopic *dc* conductivity is often a result of various electron transport processes and is, as a rule, ~$10^3$ S $m^{-1}$ for the initial disordered PAn[34,41,42,54–57] and ~$10^4$ S $m^{-1}$ for the oriented polymer.[42,58] This hampers correct studies of genuine dynamics of charge transfer along the polymer chain by conventional experimental methods, since it can be masked by interchain, interglobular, and other processes. Interpretation of experimental results is complicated by nonuniformity of the distribution of counterions.

Unlike other COP, in PAn the N heteroatom is incorporated between the phenyl rings of the chain and is a constituent of the conjugation chain, while the phenyl groups bound to the N atom can rotate about the principal axis of the macromolecule. It is these and some other peculiarities of the polymer that are responsible for the essential differences between the magnetic and electron transport properties of PAn and other COP. For instance, additional mobility of macromolecular units can modulate rather strong electron-phonon interactions and be the reason for more complicated mechanisms of electron transfer in PAn.[59] Analysis of the experimental data on temperature dependences of the *dc* conductivity, thermoelectromotive force S, and the Pauli magnetic susceptibility[60,61] made it possible to conclude that PAn · EB is an amorphous insulator whose oxidation or protonation results in the formation of 3D granulated metal-like clusters. Detailed studies of the complex dielectric constant measured at super-high frequencies (SHF), as well as analysis of the dependence of conductivity on the applied electric field,[39–42,45,49] revealed that each of the PAn · ES(A) clusters both in the initial (disordered) PAn and in the oriented PAn consists of several parallel strongly interacting chains. Charge transfer between these chains follows the 1D VRH mechanism, whereas the 3D delocalization of the electrons occurs within such clusters. The conductivity ($\sigma_{ac}$) of 3D clusters in PAn · ES(A), assessed in the framework of the Drude model, is ~$10^9$ S $m^{-1}$ [62] and appeared to be close to the value predicted for analogous clusters in *trans*-PAc.[32] However, the SHF conductivity $\sigma_{ac}$ measured at 6.5 GHz did not exceed $7 \cdot 10^4$ S $m^{-1}$.[62] This means that the actual picture of electron transfer is masked by other processes and can hardly be determined by conventional experimental techniques.

Fundamental properties of conducting polymers are to a great extent determined by paramagnetic centers (PC) with spins $S = 1/2$, localized and/or delocalized along the polymer chains. This makes it possible to use the complementary magnetic resonance methods (EPR and NMR spectroscopy) for studying the spin-lattice and spin-spin magnetic relaxation of the charge carriers.[63–65] Then, the data obtained can be used for determining the coefficients of spin diffusion along the polymer chains ($D_{1D}$) and between the polymer chains ($D_{3D}$), as well as the coefficients $A = D_{1D}/D_{3D}$ of the anisotropy of charge transfer even in a disordered polymer, at a scale beginning with several macromolecular units. It is important to know these parameters to gain a better insight into relations between the relaxation and transport properties of the spin charge carriers and the structure and dynamics of the microenvironment (the lattice, anion, *etc.*), as well as to determine the charge transfer mechanism in COP. Such studies were carried out mostly for PAn · HCl.[66–70] Previously,[65] it was reported that the experimental data obtained in the NMR studies of the proton relaxation in PAn[66,69,70] reflect the electron spin dynamics only indirectly and cannot give an unambiguous picture of charge transfer in the polymer. On the other hand, electronic relaxation of the spin charge carriers themselves is observed by EPR spectroscopy, which makes it possible to determine the relaxation and dynamic parameters of polarons in PAn and other COP more correctly.

For instance, the $D_{1D}$ values obtained by low-frequency EPR and NMR spectroscopy for fully protonated PAn · HCl is respectively equal to ~$10^{14}$ and $10^{12}$ rad $s^{-1}$. They depend only slightly on the doping level of the specimen, whereas the $D_{3D}$ values are strongly dependent on $y$ and correlate with both the *dc* and *ac* conductivity of the polymer.[66] This fact was interpreted[60,61] in favor of the existence of individual highly conducting chains with 1D electron transfer between them even in the fully protonated PAn. However, this is inconsistent with the alternative model for the formation of 3D metal-like clusters in this polymer. Additionally, the diffusion constants reported in the EPR studies on the polaron dynamics in PAn were calculated from the EPR linewidths. However, essential limitations of the EPR method manifest themselves if the recording frequency is not higher than 10 GHz. This is valid for COP as well as for other organic systems and is mainly due to the fact that the signals of free radicals are recorded in a narrow magnetic field range; this also results in the overlap of the lines of either the multiplet spectra or the spectra of different radicals with close $g$-factors. Therefore, in the general case the PAn linewidth is a superposition of different contributions

(including those due to localized and delocalized PC), which cannot be determined by conventional EPR techniques. This also results in ambiguous interpretation of the data obtained by relatively low-frequency EPR spectroscopy. Therefore, electronic relaxation, the electron dynamics, and the mechanism of charge transport in PAn and other COP are still to be clarified.

Various procedures have been developed to increase the efficiency of using EPR spectroscopy in studies of condensed media. They include the electron spin echo[71]; optical recording of EPR signal based on the spin polarization effect[72]; electron-nuclear double resonance[73,74]; methods of steady-state SHF saturation and SHF saturation transfer[75]; EPR in nonuniform fields,[76] and some other techniques. However, these procedures can be used for studying specific objects only. In this connection, operation in stronger magnetic fields and at higher recording frequencies seems to be more effective for increasing the accuracy and informativeness of the method.[77]

Previously,[79–80] we have shown that the use of EPR spectroscopy in the millimeter wave band makes it possible to obtain additional, fundamentally new information on various organic systems with paramagnetic additives including COP.[79–83] In this wave band, it is possible to determine all components of the g- and A-tensors and to perform separate determination of the spin-lattice and spin-spin relaxation times of the PC characterized by relatively weak spin-orbital interaction. Using the data obtained in this wave band, we can also calculate separately the dynamic parameters for both localized and delocalized PC and study the charge transfer process in polymer systems. The use of specially developed procedures provides a possibility for obtaining new information on the macromolecular dynamics, phase transitions, and other processes occurring in COP and related systems.

In this review, the results are generalized of original studies of the magnetic and electron transport properties of PAn · $H_2SO_4$, PAn · HCl, PAn · CS, and PAn · AMPS specimens with different conductivities and degrees of oxidation, carried out at the Institute of Problems of Chemical Physics of the Russian Academy of Sciences.[84–91] Using multifrequency EPR spectroscopy in combination with the methods of steady-state SHF saturation and SHF saturation transfer of the spin packets, as well as the spin labeling and spin probe techniques, we determined the dependences of the shape of the EPR spectra for the EB and ES forms of PAn on the composition, relaxation, and polaron mobility over a wide temperature range. Ultraslow librations of the polymer chains, which correlate with the interchain charge transfer, were recorded by the SHF saturation transfer method. By comparing the temperature dependences of the *dc* and *ac* conductivities ($\sigma_{dc}$ and $\sigma_{ac}$, respectively) we analyzed the mechanism of charge transfer in PAn depending on the anion structure and oxidation degree of the polymers.

### Polyaniline doped with sulfuric acid

Nearly symmetric Lorentzian signals are observed in the 3-cm EPR spectrum of the PAn · $H_2SO_4$ specimen with $y \leq 0.03$ (Fig. 1, spectrum *5*). The linewidths decrease as the oxidation degree of the specimen and/or the temperature increases (spectrum *6*). Computer simulation of these EPR spectra showed that at least two types of PC ($R_1$ and $R_2$) are stabilized in the unoxidized PAn. The former are localized on the polymer chain and are characterized by the anisotropic magnetic parameters $g_{xx} = 2.00535$, $g_{yy} = 2.00415$, $g_{zz} = 2.00238$, $A_{xx} = A_{yy} = 0.33$ mT, and $A_{zz} = 2.3$ mT. The latter are mobile and are characterized by the magnetic parameters $g_\perp = 2.00351$ and $g_\parallel = 2.00212$. The model spectra of radicals $R_1$ and $R_2$ are shown in Fig. 1 (spectra *1*, *2* and *3*, *4*, respectively). The PC $R_1$ and $R_2$ are located in the polymer domains respectively characterized by lesser and greater crystallinity. The $R_1$ paramagnetic centers exhibiting an asymmetric EPR spectrum can be considered as $(-Ph-N^{\cdot}H-Ph-)_n$ macroradicals localized on short segments of the polymer chain. The magnetic parameters of the $R_1$ radical differ only slightly from those of the Ph—N$^{\cdot}$—Ph radical,[92,93] which is likely due to the lower density of the unpaired electron on the nucleus of the N atom ($\rho_N^{\pi} = 0.39$) and more planar conformation of the polymer chain. According to calculations,[94] the CH groups of this radical make a relatively small contribution to $\Delta g_{xx}$ ($\sim 1.7 \cdot 10^{-3}$). The minimum energies of the spin transitions from the n- and σ-orbitals to the π*-orbital of the nitro group of the radical can be calculated using the formula[94]

$$\Delta g = \frac{g_e \lambda_{NO} \rho_N^{\pi}(0)}{\Delta E_{n\pi^*,\sigma\pi^*}}, \qquad (1)$$

where $\Delta g = g_{xx,yy} - g_{zz}$, $g_e = 2.00232$ is the g-factor of a

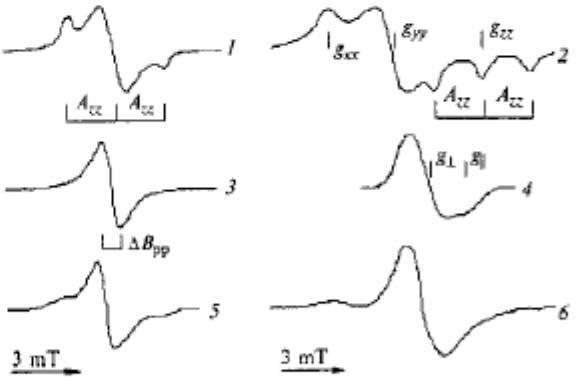


**Fig. 1.** Simulated 3-cm (*1*, *3*) and 2-mm (*2*, *4*) wave band EPR spectra of $R_1$ (*1* and *2*) and $R_2$ radicals (*3* and *4*), calculated with the parameters $g_{xx} = 2.00535$, $g_{yy} = 2.00415$, $g_{zz} = 2.00238$, $A_{xx} = A_{yy} = 0.33$ mT, $A_{zz} = 2.3$ mT, $g_\perp = 2.00351$, and $g_\parallel = 2.00212$; experimental 3-cm (*5*) and 2-mm (*6*) wave band EPR spectra of the same radicals at 300 K; $g_{ii}$, $A_{zz}$, and $\Delta B_{pp}$ are measured magnetic parameters.

free electron, and $\lambda_N$ is the constant of spin-orbital interaction of the unpaired electron with the nucleus of the N atom. For the $R_1$ radical, these values are $\Delta E_{n\pi^*} = 3.8$ eV and $\Delta E_{\sigma\pi^*} = 6.5$ eV.

Previously,[79,80] we showed that the magnetic parameters $g_{xx}$ and $A_{zz}$ of radicals containing N atoms are the most sensitive to changes in the properties, *e.g.*, the polarity and dynamics of its microenvironment in the polymer matrix. Therefore, the fact that the $g_{xx}$ value for the $R_1$ radical is shifted toward stronger fields as the oxidation degree of PAn increases can be explained not only by increase in the polarity of the radical microenvironment, but also by intensification of the motion of the radical in the $yz$ plane of its molecular system of coordinates.

The average values of the $g$-factors of the $R_1$ and $R_2$ radicals are approximately equal, *i.e.*, $\langle g\rangle_1 = (1/3)(g_{xx} + g_{yy} + g_{zz}) \approx \langle g\rangle_2 = (1/3)(g_\parallel + 2g_\perp)$. This indicates that the mobility of a fraction of radicals $R_1$ along the polymer chain increases as the oxidation degree of PAn increases. Such an "unfreezing" of the mobility results in more intense exchange between the spectral components of the PC and, hence, to a decrease in the anisotropy of its EPR spectrum. In other words, radical $R_1$ transforms into radical $R_2$, which can be considered as a polaron diffusing along the polymer chain at a minimum rate assessed by the following relation[95]:

$$\nu^0_{1D} \geq \frac{(g_{xx} - g_e)\mu_B B_0}{2\pi\hbar}, \qquad (2)$$

where $\mu_B$ is the Bohr magneton, $B_0$ is the resonance magnetic field, and $\hbar$ is the Planck constant. Using the $g_{xx}$ value for the EB form of PAn (see above), for this polymer we get $\nu^0_{1D} \geq 5.7 \cdot 10^7$ s$^{-1}$.

If the oxidation degree $y$ exceeds 0.03, the EPR spectrum of PAn transforms into the singlet spectrum recorded at $g = 2.00303$ (Fig. 2). In the 2-mm wave band, the specimen with the highest degree of oxidation exhibits an asymmetric spectrum with the Dysonian lineshape characteristic of PC in highly conducting inorganic[96] and organic single crystals[97] and polymers.[64,65,79,98–101]

The EPR spectrum has a contribution of the dispersion signal due to the formation of the skin layer and is characterized by the asymmetry factor $A/B$ (see Fig. 2). Therefore, correct determination of the relaxation and magnetic resonance parameters of such PC requires simulation of their EPR spectra. The overall spectrum of the highly conducting PAn specimen was calculated assuming that the skin layer depth $\delta$ is close to the characteristic size $d$ of the polymer particle (*i.e.*, at $d/2\delta \approx 1$) using the equation for the first derivative of the signal containing the contributions $D$ and $A$ of the dispersion and absorption signals, respectively,[102]

$$d\chi/dB = D\frac{1 - x^2}{(1 + x^2)^2} + A\frac{2x}{(1 + x^2)^2}, \qquad (3)$$

where $x = (B - B_0) \cdot T_{r2}$, $T_{r2} = 2/(\sqrt{3}\gamma_e \Delta B_{pp})$ is the spin-spin relaxation time; $\gamma_e$ is the gyromagnetic ratio of the electron, and $\Delta B_{pp}$ is the peak-to-peak EPR linewidth. Figure 2 (spectrum *2*) illustrates an example of calculations of the 2-mm wave band EPR spectrum. Variations of the lineshape and magnetic parameters of PC indicate strengthening of the spin-spin interaction and intensification of the spin dynamics on oxidation of PAn.

The EPR spectra of PAn ($y \geq 0.22$) recorded in the 3-cm wave band exhibit a hyperfine structure (HFS), which is due to the interaction of a small fraction of unpaired electrons with the protons of the benzene rings and with the nucleus of the N atom. The HFS components have low relative intensities. The central portions of the second harmonic curves of the absorption signals for two specimens of PAn · $H_2SO_4$ (with $y = 0.22$ and 0.53) are shown in Fig. 3 as examples. In the first specimen, the interaction of the unpaired electron with

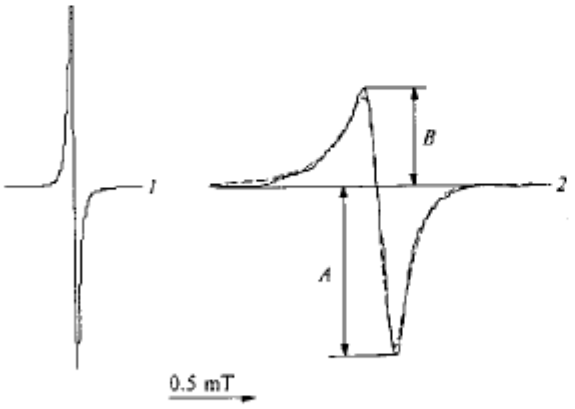


**Fig. 2.** Typical 3-cm (*1*) and 2-mm (*2*) wave band EPR spectra of polyaniline with the degree of oxidation $y = 0.53$ at room temperature. The measured values $A$ and $B$ are shown. The spectrum calculated using Eq. (3) with $L = D/A = 0.58$ or $A/B = 1.84$ and $(\sqrt{3}/2)\Delta B_{pp} = (T_{r2}\gamma_e)^{-1} = 0.15$ mT is shown by the dashed line.

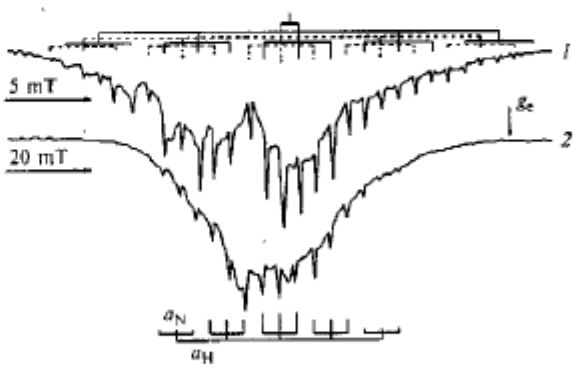


**Fig. 3.** Central portions of the curves of the second derivative of the in-phase 3-cm wave band absorption signals of polyaniline with the oxidation levels $y = 0.53$ (*1*) and 0.22 (*2*), recorded at room temperature. The HFS are shown and the constants of HFI of the unpaired electron with the nuclei of H ($a_H$) and N ($a_N$) atoms are presented; the position of the $g$-factor of free electron ($g_e = 2.00232$) is also shown.

four neighboring nearly equivalent protons (spin $I = 1/2$) of the side phenyl groups and with the central nucleus of the N atom (the nuclear spin $I = 1$) gives rise to HFS with well-resolved equidistant components with the ratio of intensities 1 : 5 : 11 : 14 : 11 : 5 : 1 (see Fig. 3, spectrum *2*). In addition to the above-mentioned nuclei, in the second PAn · $H_2SO_4$ specimen ($y = 0.53$) the unpaired electron also begins interacting with the proton located at the central N atom. This results in additional splitting in the absorption spectrum of the specimen. The hyperfine interaction (HFI) constant $a_H$ varies in the range from 5.0 to 9.6 μT for different PAn · $H_2SO_4$ specimens; however, these variations do not correlate with those of $y$. In these polymers, the spin density on the protons ($\rho_H^\pi$), determined from the well-known McConnel relationship $a_H = Q_H\rho_H^\pi$, lies in the range $(2.2–4.3) \cdot 10^{-3}$ at $Q_H = 2.25$ mT for the benzene anion.[103] This value differs from that found for solution of the EB form of PAn in dioxane ($\rho_H^\pi = 1.5 \cdot 10^{-2}$),[104] in which the unpaired electron interacts with two side benzene rings of the PAn molecule. This suggests a greater spin delocalization along the polymer chain and a more planar conformation of the polymer chains in the PAn specimens studied.

The fact that both the *dc* conductivity $\sigma_{dc}$ and the paramagnetic susceptibility $\chi_{pm}$ obtained in the 3-cm EPR wave band depend in a similar manner on the degree of oxidation ($y$) of PAn · $H_2SO_4$ (Fig. 4) indicates that the *dc* conductivity of the polymer is to a great extent determined by the number and dynamics of PC. Oxidation of the specimen is accompanied by the formation of metal-like clusters with 3D-delocalized electrons.[46,47] This is confirmed by the data obtained previously by electron microscopy and X-ray diffraction,[85] as well as by the above-mentioned changes in the magnetic parameters, the shape of the spectrum, and the conductivity observed on oxidation of PAn, especially above the percolation threshold with $y \geq 0.22$.

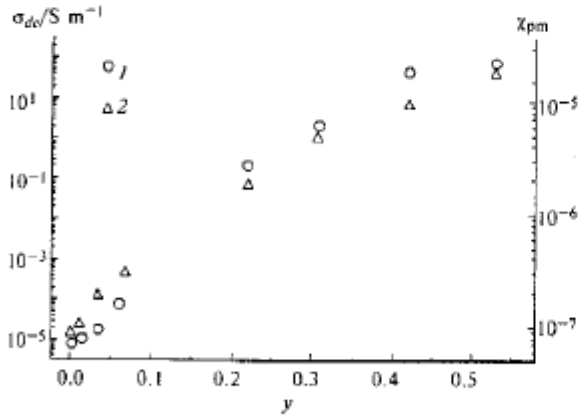


**Fig. 4.** Dependences of $\sigma_{dc}$ (*1*) and $\chi_{pm}$ (*2*) of PAn specimens on the degree of oxidation $y$ at 300 K.

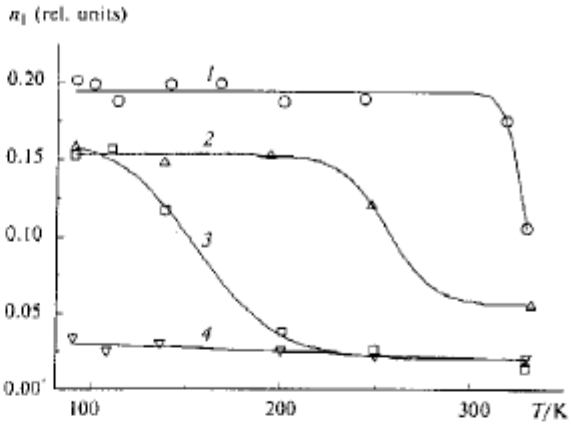


**Fig. 5.** Temperature dependences of the relative concentration $n_l$ of radicals $R_1$ localized on the polymer chain in specimens of PAn with $y = 0$ (*1*), ~0.01 (*2*), ~0.03 (*3*), and 0.22 (*4*).

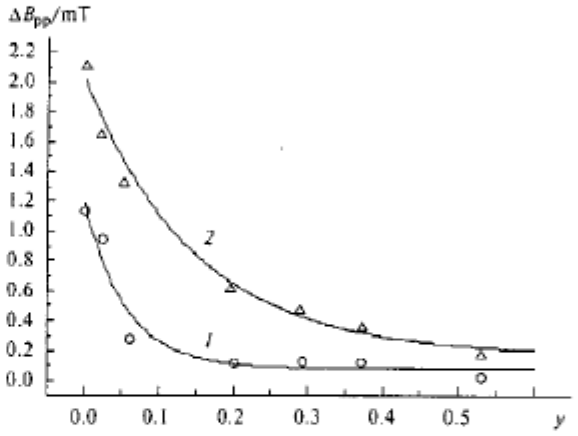


**Fig. 6.** Dependences of the linewidth $\Delta B_{pp}$ of radicals $R_2$ in the 2-mm (*1*) and 3-cm (*2*) wave band EPR spectra on the degree of PAn oxidation $y$ at room temperature.

The relative concentration $n_l$ of localized polarons of the $R_1$ type in specimens with different oxidation degrees varies with temperature (Fig. 5). For radicals of the $R_2$ type, the linewidths $\Delta B_{pp}$ measured in the 3-cm and 2-mm EPR wave bands decrease as $y$ increases (Fig. 6). This indicates that the effective spin-spin relaxation time becomes shorter due to the formation in the specimen of domains with high spin density and fast exchange between spin packets. The spin concentration is much lower than the concentration of charge carriers in PAn · ES(A). This can be due to the fact that a fraction of paramagnetic polarons collapses into diamagnetic bipolarons above the percolation threshold of the polymer at $y \geq 0.02$.

Not only the narrowing of the EPR line of $R_2$ radicals, but also a decrease in their $g$-factor, occurs on oxidation. This effect can be due to a decrease in the

spin density on the $^{14}N$ nucleus (see Eq. (1)), as well as to the change in the conformation of the polymer chains. It is known[45] that the —Ph—N—Ph— angle can change by 22° upon doping of PAn. However, calculations showed[79] that such a change in the angle must result in a decrease in the $g_{\perp}$ value by several percent only. The above-mentioned change in the spectroscopic parameters is likely due to the decrease in the θ dihedral angle between the planes of the neighboring benzene rings in the Ph—N—Ph fragment, occurring on doping. The transfer integral $I_{C-H}$ between the $p_z$-orbitals of the N and C atoms in the *para*-positions with respect to the benzene rings of PAn depends on the dihedral angle as $I_{C-H} \propto \cos\theta$,[106,107] which is typical of aromatic hydrocarbons. Assuming that the θ angle in the EB form of PAn is 56°,[107] one can calculate for the ES(A) form of PAn ($y = 0.22$) the effective dihedral angle θ and the spin density on the N atom $\rho_N^{\pi}(0)$, which are equal to 33° and to 0.42, respectively. Such a decrease in the θ angle results in increase in the spin density on the benzene rings due to an increase in the transfer integral $I_{C-H}$. Thus, the observed changes in the magnetic parameters may indicate a greater spin delocalization along the polymer chain as well as an increase in the polymer chain planarity owing to oxidation.

Appreciable weakening of the exchange interaction between individual spin packets is due to increase in both the recording frequency and the strength of the external magnetic field.[108] Therefore, operation in the 2-mm EPR wave band must lead to saturation of the spin packets under conventional experimental conditions. In fact, as for other COP,[79,81—83] both the in-phase and quadrature components of the dispersion signals of neutral and weakly oxidized PAn, recorded in the 2-mm wave band, contain bell-shaped components with Gaussian spin packet distributions (Fig. 7). This was not observed in the studies of COP at lower frequencies. This type of components is a result of rapid passage of PC carried out where the conditions hold of (i) the spin packet saturation $\gamma_e B_1 \sqrt{T_{r1}T_{r2}} > 1$ and (ii) adiabatic passage of resonance $dB/dt = B_m\omega_m < \gamma_e B_1^2$, where $T_{r1}$ and $T_{r2}$ are, respectively, the spin-lattice and spin-spin relaxation time, $dB/dt$ is the rate of passage of resonance, $B_m$ and $\omega_m$ are the amplitude and angular frequency of magnetic field modulation, respectively, and $B_1$ is the magnetic component of the polarizing SHF field.

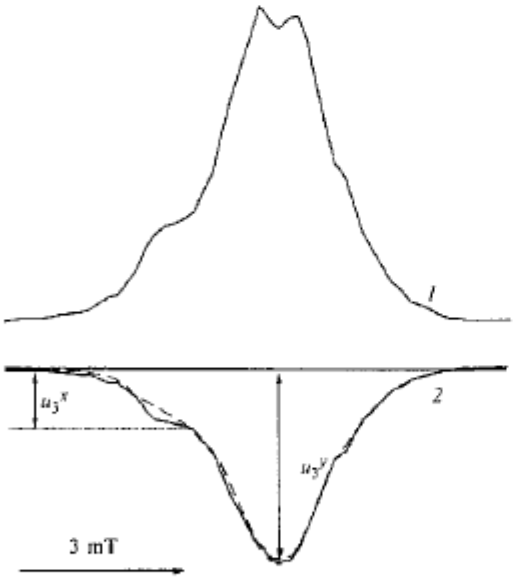


**Fig. 7.** Typical spectra of the in-phase (*1*) and quadrature (*2*) components of the 2-mm wave band EPR dispersion signal of PAn with the degree of oxidation $y \le 0.03$ at room temperature. The measured components ($u$) of the quadrature dispersion spectrum are shown.

The equation for the first derivative of the dispersion signal can be written in the general form[109]

$$U = u_1 g'(\omega_e)\sin(\omega_m t) + u_2 g(\omega_e)\sin(\omega_m t - \pi) + u_3 g(\omega_e)\sin(\omega_m t \pm 0.5\pi). \quad (4)$$

Obviously, $u_2 = u_3 = 0$ in the absence of SHF saturation. In the case of SHF saturation the relative intensities of the $u_1$ and $u_3$ components are determined by the ratio of the effective relaxation rate of spin packets $\tau^{-1} = (T_{r1}T_{r2})^{-1/2}$ and the rate of passage of resonance $\omega_m B_m$. If the latter is high and the modulation frequency is comparable with or higher than $\tau^{-1}$, the spin packets have no time to track the reverse of the direction of the passage of the magnetic field because it proceeds at too high a rate. In the case of adiabatic passage of resonance (if $\omega_m B_m \ll \gamma_e B_1^2$) each spin can "see" only an averaged applied magnetic field; therefore, the first derivative of the dispersion signal will be mainly determined by the last two terms of Eq. (4), where $u_2 = (\chi_0\pi\gamma_e^2 B_1 B_m T_{r2})/2$ and $u_3 = (\chi_0\pi\gamma_e^2 B_1 B_m T_{r2})/(4\omega_m T_{r1})$.

If the effective spin relaxation time is shorter than the modulation period ($\tau < \omega_m$) and $\tau > B_1/(dB/dt)$, the magnetization vector has sufficient time to recover to the equilibrium state during one modulation period. In this case the dispersion signal should be independent of the recording frequency and will be mainly determined by the $u_1 g'(\omega_e)$ and $u_3 g(\omega_e)$ terms of Eq. (4), where $u_1 = \chi_0\pi\gamma_e^2 B_1 B_m$ and $u_3 = (\chi_0\pi\gamma_e^2 B_1 B_m T_{r1}T_{r2})/2$. Thus the electronic relaxation times of the spin system can be determined from the components of the dispersion signal of saturated spin packets, recorded at corresponding phase tuning of the synchronous detector using the following equations[110]:

$$T_{r1} = \frac{3\omega_m(1+6\Omega)}{\gamma_e^2 B_{1_0}^2 \Omega(1+\Omega)}, \quad (5a)$$

$$T_{r2} = \Omega/\omega_m \quad (5b)$$

(here $\Omega = u_3/u_2$ and $B_{1_0}$ is the strength of the polarizing field at $u_1 = -u_2$) at $\omega_m^0 T_{r1} > 1$ and

$$T_{r1} = \frac{\pi u_3}{2\omega_m u_1}, \quad (6a)$$

$$T_{r2} = \frac{\pi u_3}{2\omega_m (u_1 + 11u_2)} \quad (6b)$$

at $\omega_m T_{r1} < 1$. The amplitudes of the $u_i$ components are measured at the center of the spectrum (at $\omega = \omega_c$).

The increase in the degree of oxidation of the polymer leads to shortening of the effective relaxation time of PC (Fig. 8), which can be due to intensification of the spin exchange with the lattice and with other spins stabilized on neighboring polymer chains of highly conducting clusters. In this connection it should be noted that electronic relaxation processes occurring in condensed media at high temperatures are mainly determined by the Raman interaction between the electron and the optical phonons of the lattice. The probability and rate of such processes are dependent on the concentration $n$ of the PC localized, *e.g.*, in ionic crystals ($W_R \propto T_{r1}^{-1} \propto n^2 T^7$) and in π-conjugated polymers ($W_R \propto T_{r1}^{-1} \propto nT^2$).[111] The available data suggest that the $T_{r1}^{-1}$ values of PC in polyaniline (with $y \leq 0.02$) are described by a dependence of the type $T_{r1}^{-1} \propto nT^{-k}$, where $k = 3$—4, whereas those of PC in the polymer with $y = 0.22$ are described by a flattened dependence characterized by the opposite sign of temperature variations, $T_{r1}^{-1} \propto nT^{0.3}$ (see Fig. 8). This indicates the appearance of an additional channel of the energy transfer from the spin ensemble to the lattice on oxidation of the polymer, as is the case in the classical metals.

The amplitude and shape of the components of the dispersion signal depend not only on the intensity of spin exchange and the rate of electronic relaxation, but also on relatively slow macromolecular reorientations (librations, torsional vibrations) in the polymer. Usually, such motions are studied by EPR spectroscopy with SHF saturation transfer (ST EPR) between the spin packets differently oriented with respect to the external magnetic field.[75] The use of the ST EPR method makes it possible to study torsional motions of the macromolecule (*e.g.*, with respect to its principal $x$ axis) with correlation times $\tau_c$ varied from $10^{-7}$ s to the maximum value given by the formula[75]

$$\tau_c^{max} = \frac{2}{3\pi^2 T_1 \gamma_e^2 B_1^4} \cdot \frac{\sin^2\vartheta \cos^2\vartheta \left(B_\perp^2 - B_\parallel^2\right)^2}{B_\perp^2 \sin^2\vartheta + B_\parallel^2 \cos^2\vartheta}, \quad (7)$$

where $B_\parallel$ and $B_\perp$ are the positions of the high- and low-field spectral components, respectively, and $\vartheta$ is the angle between the direction of the external magnetic field $B_0$ and that of the $x$ axis of the macromolecule.

Temperature variation of the relative intensity of the high-field $u_3$ component of the quadrature dispersion signal (see Fig. 7) is a typical manifestation of intensification of ultraslow (and anisotropic with respect to the $x$ axis) librations of macromolecules carrying localized $R_1$ radicals. Previously,[79,80] we have shown that the use of the 2-mm wave band ST EPR makes it possible to separately determine the main characteristic times $\tau_c$, $T_{r1}$, and $T_{r2}$ of the radicals involved in the ultraslow anisotropic motions with respect to different molecular axes. The correlation time $\tau_c^x$ of the ultraslow motions of PC about the $x$ axis can be determined from the ratio of the intensities of the $u_3$ components of the anisotropic spectrum, $K_{mov} = u_3^x/u_3^y$, using the following equation[79,86]:

$$\tau_c^x = \tau_c^0 \left(\frac{u_3^x}{u_3^y}\right)^{-\alpha}, \quad (8)$$

where the constant α is determined by the anisotropy of the $g$-factor of PC. The Arrhenius dependence of the correlation time of macromolecular librations in the initial PAn specimen, calculated using Eq. (8) at $\tau_c^0 = 5.4 \cdot 10^{-8}$ s and $m = 4.8$, is shown in Fig. 9. As can be seen, the low-temperature branch of this dependence is satisfactorily described by the relationship $\tau_c = 2.7 \cdot 10^{-7} \exp(0.045\ \text{eV}/k_B T)$, where $k_B$ is the Boltzmann constant. Analogous dependences were obtained for PAn · $H_2SO_4$ with the oxidation levels $y \cong 0.01$ and $y \cong 0.03$. The calculated activation energies of macromolecular librations correspond to the energies of optical phonons and are close to the value (0.01—0.03 eV)[112] obtained for different specimens of poly(tetrathiafulvalenes)[113,114] and poly(bis)alkylthioacetylene.[115] The $\tau_c^{max}$ time calculated using Eq. (7) with the parameters $\vartheta = 45°$ and $B_1 = 0.01$ mT[79,80] and the $g_{xx}$ and $g_{zz}$ values for $R_1$ radicals is $2.2 \cdot 10^{-4}$ s and corresponds to a $u_3^x/u_3^y$ ratio of 0.2 (see Eq. (8)) at 100 K. The increase in the correlation time on heating of the polymer above the critical temperature ($T_c \approx 190$ K) is still to be clarified.

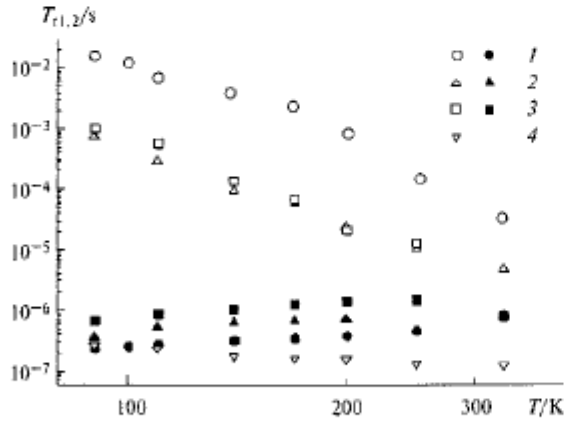


**Fig. 8.** Temperature dependences of the effective spin-lattice and spin-spin relaxation times ($T_{r1}$, open circles and $T_{r2}$, filled circles, respectively) of PAn specimens with $y = 0$ (*1*), ~0.01 (*2*), ~0.03 (*3*), and 0.22 (*4*).

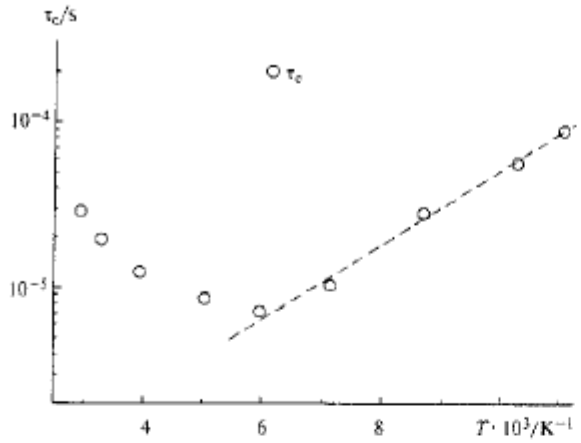


**Fig. 9.** The Arrhenius dependence of the correlation time of ultraslow cooperative librations of paramagnetic centers $R_2$ and the polymer chain. The dependence calculated using the equation $\tau_c = \tau_c^0 \exp(0.045 \text{ eV}/k_B T)$ with $\tau_c^0 = 2.7 \cdot 10^{-7}$ s is shown by the dashed line.

The relaxation times of the electron and proton spins in PAn vary depending on the recording frequency as $T_{r1,2} \propto n^{-1}\nu^{1/2}$ ($\omega = 2\pi\nu$).[66,70] In this connection the experimental data obtained can be explained by modulation of electronic relaxation by 1D diffusion of $R_2$ radicals along the polymer chain and by 3D hopping of these radicals between the chains with the diffusion coefficients $D_{1D}$ and $D_{3D}$, respectively. In this case, the spectral density function for the spin mobility in the 1D system can be written as[116]

$$J(\omega) = n\phi(\omega)\Sigma_{ij}, \qquad (9)$$

where $n = (n_1 + n_2)/\sqrt{2}$ is the effective concentration of both localized and delocalized PC per monomer unit of PAn, $n_1$ and $n_2$ are the relative concentrations of localized and delocalized PC, respectively, $\Sigma_{ij}$ is the lattice sum for the powder-like specimen,

$$J_{1D}(\omega) = \frac{1}{\sqrt{2D_{1D}D_{3D}}} \sqrt{\frac{\sqrt{1 + \sqrt{1 + (\omega/D_{3D})^2}}}{1 + (\omega/D_{3D})^2}} =$$

$$\begin{cases} (2D'_{1D}\omega)^{-1/2}, & \text{at } D'_{1D} >> \omega >> D_{3D}, \\ (2D'_{1D}D_{3D})^{-1/2}, & \text{at } \omega << D_{3D}, \end{cases}$$

$D'_{1D} = 4D_{1D}/N^2$, and $N$ is the spin delocalization length in the monomer units. Previously,[66–70] an analogous spectral density function was used in the studies of the spin dynamics in PAn.

Since the electronic relaxation is mainly determined by the dipole-dipole interaction between localized and delocalized spins (with a spin value $S = 1/2$), we can write the following equations for the rates of electronic relaxation[117]:

$$T_{r1}^{-1} = \langle\omega^2\rangle[2J(\omega) + 8J(2\omega)], \qquad (10a)$$

$$T_{r2}^{-1} = \langle\omega^2\rangle[3J(0) + 5J(\omega) + 2J(2\omega)], \qquad (10b)$$

where $\langle\omega^2\rangle = 0.1(\mu_0/4\pi)^2\gamma_e^2\hbar^2S(S+1)n\Sigma_{ij}$ is the averaged constant of the spin dipole interaction for a powder-like specimen.

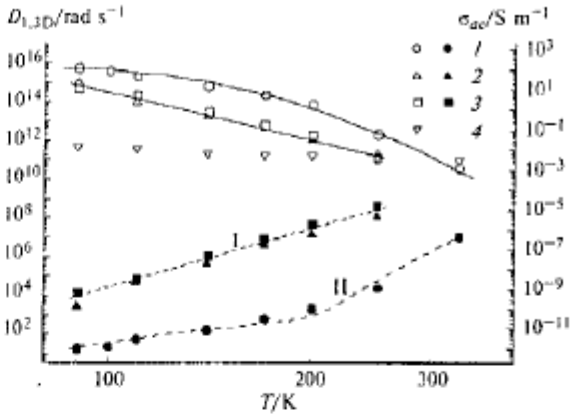


**Fig. 10.** Temperature dependences of the coefficients of the polaron diffusion along the polymer chain $D_{1D}$ (open circles) and of the interchain polaron hopping $D_{3D}$ (filled circles) in PAn with $y = 0$ (*1*), ~0.01 (*2*), and ~0.03 (*3*); temperature dependence of the effective coefficient of the polaron diffusion in polyaniline with $y = 0.22$ (*4*). The functions $\sigma_{1D}(T) \propto \sigma_{ac}(T)$ calculated using Eq. (14b) with the parameters $m = 12.9$ and $\sigma_{ac}^0 = 2.8 \cdot 10^{-12}$ S m$^{-1}$ s K (*1*); $m = 12.6$ and $\sigma_{ac}^0 = 8.8 \cdot 10^{-14}$ S m$^{-1}$ s K (*2*, *3*), and $k_3 = 1 \cdot 10^{24}$ s K$^{m+1}$ are shown by solid lines. The functions $\sigma_{3D}(T) \propto \sigma_{ac}(T)$ calculated using Eq. (13b) (with $\sigma_{ac}^0 = 1.4 \cdot 10^{-11}$ S m$^{-1}$ s$^{0.8}$ K$^{-1}$ and $E_a = 0.13$ eV, curve I) and with the parameters $\sigma_{ac}^0 = 1.2 \cdot 10^{-12}$ S m$^{-1}$ s$^{0.8}$ K$^{-1}$ and $E_a = 0.035$ eV (at $T \le 240$ K) and with $\sigma_{ac}^0 = 5.7 \cdot 10^{-3}$ S m$^{-1}$ s$^{0.8}$ K$^{-1}$ and $E_a = 0.43$ eV (at $T \ge 240$ K) (curve II) are shown by dashed lines.

The temperature dependences of the effective dynamic parameters $D_{1D}$ and $D_{3D}$ for both types of radicals in several PAn specimens (see Fig. 10) were calculated from the data presented in Fig. 8 using Eqs. (9) and (10) at $N \approx 5$.[118] It seems to be justified that the anisotropy of the spin dynamics is maximum in the initial specimen of the EB form of PAn and decreases as $y$ increases. At a relatively high degree of oxidation ($y \ge 0.22$), the electronic relaxation times become comparable and only slightly temperature-dependent because of intense spin-spin exchange in metal-like clusters and of the increase in the effective dimensionality of the system.

It was found by EPR spectroscopy at recording frequencies from 5 to 450 MHz[66,70] that fairly high

anisotropy of the spin dynamics is retained in PAn · HCl oxidized up to $y = 0.6$ even at room temperature. However, our experimental data indicate that the anisotropy of the motion of the charge carriers is high only in the oxidized PAn · $H_2SO_4$ for which $y < 0.22$. Such a discrepancy is likely due to the fact that the effective dimensionality of PAn doped with $H_2SO_4$ to $y \geq 0.22$ is larger than that of PAn · HCl. The increase in the dimensionality on oxidation of the polymer is accompanied by a decrease in the number of electron traps, which reduces the probability of electron scattering by the lattice phonons and results in the virtually isotropic spin motion and relatively slight temperature dependences of both the electronic relaxation and diffusion rates of PC, as is the case for amorphous inorganic semiconductors.[20,29]

As was mentioned above, EPR spectroscopy makes it possible to study the spin dynamics and conductivity at the scale of several polymer chains. In principle, the macroscopic and microscopic conductivity ($\sigma_{dc}$ and $\sigma_{ac}$, respectively) can correlate; however, if the oxidized polymer contains a sufficient amount of diamagnetic bipolarons, these parameters should be appreciably different. Therefore the conductivity parameters obtained by different methods can be compared only qualitatively. If the diffusion coefficients of both the spin and spinless charge carriers in oxidized PAn ($y > 0.22$) are close, the contribution to the conductivity of the motion of bipolarons should be comparable or even greater than that of the spin charge carriers.

Let us consider the possibility of determining the high-frequency conductivity and the mechanism of charge transport in PAn.

To determine the conductivity components of a specimen due to the mobility of the spin charge carriers, one can use the known expression

$$\sigma_{1,3D}(T) = \frac{Ne^2 D_{1,3D} c_{1,3D}^2}{k_B T}, \qquad (11)$$

where $T$ is temperature, and $c_{1D} = 0.960$ nm and $c_{3D} = 0.590$ nm are the lattice constants of PAn · $H_2SO_4$.[49] At room temperature and $0 \leq y \leq 0.022$, the "along-the-chain" conductivity $\sigma_{1D}$ of oxidized PAn is 10.2 S m$^{-1}$. The $\sigma_{3D}$ component increases from $7.1 \cdot 10^{-4}$ to 0.35 S m$^{-1}$ under the same conditions. This is additional evidence for a decrease in the anisotropy of the spin motion in PAn · ES(A) and is in agreement with the conclusions drawn previously.[114]

The data on the spin dynamics can be interpreted using different models for the charge transfer in low-dimensional systems. Previously,[85] we have shown that dynamic processes occurring in PAn · ES(A) with $y \geq 0.22$ can be interpreted in the framework of the Mott model of interchain VRH of the charge carriers.[29] According to this model, the conductivity components of a disordered solid of dimensionality $d$ are defined by the following equations:

$$\sigma_{dc}(T) = \sigma_0 \exp\left[-\left(\frac{T_0}{T}\right)^{1/(d+1)}\right], \qquad (12a)$$

$$\sigma_{ac}(T) = (2/3)\pi^2 e^2 k_B T n^2(\varepsilon_F)\langle L\rangle^5 \nu_c \left(\ln\frac{\nu_0}{2\pi\nu_c}\right)^4 = \sigma_0 T, \quad (12b)$$

where $\sigma_0 = 0.39\nu_0 e^2[n(\varepsilon_F)\langle L\rangle/(k_B T)]^{1/2}$ at $d = 1$ and $\sigma_0 = 1.8\nu_0 e^2 n(\varepsilon_F) T_0/(T\langle L\rangle)$ at $d = 3$; $\nu_0$ is the limiting hopping frequency; $T_0^{-1}/\mathrm{K} = 0.62 k_B n(\varepsilon_F)\langle L\rangle^3$ is the percolation constant or the effective energy difference between the localized states, which is dependent on the degree of order of the amorphous domains of the polymer (see Eq. (12a)); and $\langle L\rangle = (L_\parallel L_\perp^2)^{1/3}$, where $\langle L\rangle$, $L_\parallel$, and $L_\perp$ are, respectively, the average localization length of the wave function of the charge carrier and its projections on the parallel and perpendicular directions. According to Eqs. (12a,b), an approximately quadratic $\sigma_{dc}(T)$ dependence and linear $\sigma_{ac}(T)$ dependence should be observed in the framework of the VRH model. Stronger temperature dependences of the conductivity of weakly oxidized PAn · $H_2SO_4$ can be interpreted in the framework of the model for the activation charge transfer between the polymer chains,[29] according to which the following equations are valid for the components of the overall conductivity:

$$\sigma_{dc}(T) = \sigma_{dc}^0 \exp\left(-\frac{E_a}{k_B T}\right), \qquad (13a)$$

$$\sigma_{ac}(T) = \sigma_{ac}^0 \nu_c^{0.8} T \exp\left(-\frac{E_a}{k_B T}\right), \qquad (13b)$$

where $E_a$ is the activation energy of electron transfer between the polymer chains.

In fact, function (13b) with the parameters $\sigma_{ac}^0$ and $E_a$ fits fairly well the experimental $D_{3D}(T)$ dependences for the initial specimen ($\sigma_{ac}^0 = 1.2 \cdot 10^{-12}$ S m$^{-1}$ s$^{0.8}$ K$^{-1}$, $E_a = 0.035$ eV) and for the specimens with $y \geq 0.01$ ($\sigma_{ac}^0 = 5.7 \cdot 10^{-3}$ S m$^{-1}$ s$^{0.8}$ K$^{-1}$, $E_a = 0.43$ eV) and $y \geq 0.03$ ($\sigma_{ac}^0 = 1.4 \cdot 10^{-11}$ S m$^{-1}$ s$^{0.8}$ K$^{-1}$, $E_a = 0.13$ eV). In the case of activation charge transfer between the polymer chains the $\sigma_{dc}(T)$ dependence should be linear. However, it is essentially nonlinear for the above-mentioned PAn · ES(A) specimens, which suggests another mechanism of charge transfer in this polymer.

The fact that the spin-lattice relaxation time of PAn is strongly dependent on temperature (see above) means that, in accord with the energy conservation law, the electron hops should be accompanied by absorption or emission of a minimum number of the lattice phonons. Multiphonon processes become predominant in neutral and weakly oxidized PAn because of a strong spin-lattice interaction. For this reason,

electrodynamic processes occurring in the polymer can be considered in the framework of Kivelson's formalism[25] of isoenergetic electron transfer between the polymer chains involving optical phonons. According to this model, Coulomb interaction occurs between the charge carriers and the dopant anions introduced into the polymer. In this case, the excess charge can be isoenergetically transferred from one charge carrier to another charge carrier moving along the neighboring polymer chain. The temperature dependence of the probability of this process and, hence, of the charge carrier mobility will be determined by the probability of finding the neutral soliton or polaron near the dopant anion. The *dc* and *ac* conductivities will be defined by the following expressions[25,38]:

$$\sigma_{dc}(T) = \frac{k_1 e^2 \gamma(T) \xi \langle y \rangle}{k_B T N_i R_0^3} \exp\left(\frac{2k_2 R_0}{\xi}\right) = \sigma_0 T^m, \qquad (14a)$$

$$\sigma_{ac}(T) = \frac{N_i^2 e^2 \langle y \rangle \xi_\parallel^3 \xi_\perp^2 \nu_e}{384 k_B T} \left(\ln \frac{2\nu_e L}{\langle y \rangle \gamma(T)}\right)^4 =$$

$$= \frac{\sigma_0 \nu_e}{T} \left(\ln \frac{k_3 \nu_e}{T^{m+1}}\right)^4, \qquad (14b)$$

where $k_1 = 0.45$; $k_2 = 1.39$; $k_3$ is a constant; $\gamma(T) = \gamma_0 (T/300\ \mathrm{K})^{m+1}$ is the rate of electron transfer between the charge carriers; $\langle y \rangle = y_p y_{bp} (y_p + y_{bp})^{-2}$, where $y_p$ and $y_{bp}$ are, respectively, the concentrations of polarons and bipolarons per monomer unit of the polymer chain; $R_0 = (4\pi N_i/3)^{-1/3}$ is the typical distance between the dopant anions with the concentration $N_i$; $\xi = (\xi_\parallel \xi_\perp^2)^{1/3}$, $\xi_\parallel$, and $\xi_\perp$ are the averaged localization length of the wave function of the charge carrier and its parallel and perpendicular components, respectively; $L$ is the number of monomer units in the polymer chain; and $m \approx 10$.

Theoretical functions $\sigma_{ac}(T) \equiv \sigma_{1D}(T)$ calculated using Eq. (14b) fit well the experimental $D_{1D}(T)$ dependences (see Fig. 10). Taking into account the dependence $\sigma_{dc}(T) \propto T^m$ for polyaniline with $0 < y \le 0.03$, one can conclude that the above-mentioned mechanism of charge transfer can be realized in these specimens. Using the known method,[26] we can assess the $\sigma_{ac}/\sigma_{dc}$ ratio for the limiting case $\omega/2\pi = \nu_e \to \infty$. The value found for PAn · $H_2SO_4$ is ~130, which is appreciably smaller than that obtained for *trans*-PAc ($\sigma_{ac}/\sigma_{dc} \equiv 10^4$).[26]

The temperature dependence of the *ac* conductivity of PAn · $H_2SO_4$ with $y = 0.22$ (Fig. 11) calculated from the data presented in Fig. 10 using Eq. (11) cannot be interpreted in the framework of the Kivelson theory of isoenergetic charge transfer since this theory assumes a stronger temperature dependence (see Fig. 10 and Eq. (14b)). The model of charge carrier scattering by optical phonons of the lattice of metal-like clusters in π-conjugated COP[32,119] may appear to be more convenient for explanation of such behavior of the conductivity. In the framework of this model the conductivity of the polymer can be expressed in the form

$$\sigma(T) = \frac{Ne^2 c_{1D}^2 M t_0^2 k_B T}{8\pi\hbar^3 \alpha^2} \cdot \left[\sinh\left(\frac{2\pi\hbar\nu_{ph}}{k_B T}\right) - 1\right] =$$

$$= \sigma_0 T \left[\sinh\left(\frac{2\pi\hbar\nu_{ph}}{k_B T}\right) - 1\right], \qquad (15)$$

where $M$ is the mass of a CH or NH group, $t_0$ is the transfer integral equal to ~2—3 eV for the π-electron, $\nu_{ph}$ is the frequency of the optical phonon, and $\alpha$ is the constant of electron-phonon interaction (for *trans*-PAc, $\alpha = 4.1 \cdot 10^{10}$ eV m$^{-1}$).[32] As can be seen in Fig. 11, the $\sigma_{ac}(T)$ dependence for a PAn · $H_2SO_4$ specimen ($y = 0.22$) is fairly well fitted using Eq. (15) with the parameters $\sigma_0 = 0.12$ S m$^{-1}$ K$^{-1}$ and the energy of the lattice phonons $2\pi\hbar\nu_{ph} = 0.033$ eV. The latter value is close to the activation energy of macromolecular anisotropic librations (see above). Using Eq. (15) with the parameters $N = 2.2 \cdot 10^{26}$ m$^{-6}$ and $c_{1D} = 0.96$ nm,[49] we get $\alpha = 1.8 \cdot 10^{12}$ eV m$^{-1}$. The *ac* conductivity of clusters in PAn · $H_2SO_4$ oxidized to $y = 0.22$ is ~60 S m$^{-1}$ at room temperature (see Fig. 11), which is much smaller than that calculated for fully oxidized PAn ($\sigma_{ac} \ge 10^9$ S m$^{-1}$).[62]

Let us calculate the *ac* conductivity of a fully oxidized polymer using the dependence of the $D$ and $A$ values (see Eq. (3)) on the recording frequency and conductivity of the polymer[120]

$$D = \frac{1}{p^2 + q^2} \cdot \frac{q \sinh p - p \sin q}{\cosh p + \cos q} + \frac{\sinh p \sin q}{(\cosh p + \cos q)^2}, \qquad (16a)$$

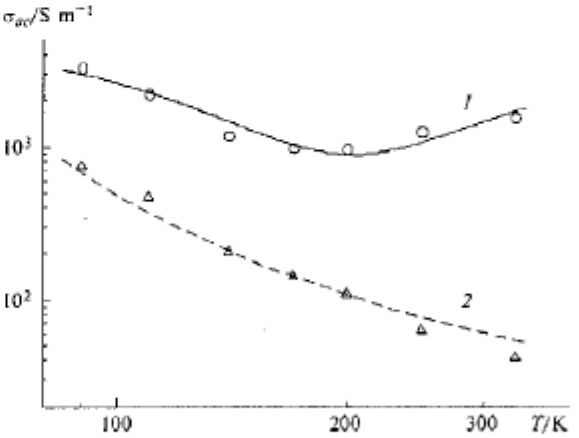


**Fig. 11.** Temperature dependences of the *ac* conductivity at $\nu_e$ = 140 GHz of PAn specimens with $y = 0.22$ (*1*) and 0.53 (*2*), calculated using Eqs. (10), (3) and (16). The dependence calculated using Eq. (17) (with $\sigma_0^{(1)} = 6.8 \cdot 10^3$ S m$^{-1}$, $\sigma_0^{(2)} = 43.5$ S m$^{-1}$ K$^{-1}$, $\sigma_0^{(3)} = 6.9$ S m$^{-1}$ K$^{-1}$, and $\hbar\nu_{ph} = 0.047$ eV) is shown by the solid line and that calculated using Eq. (15) (with $\sigma_0 = 0.12$ S m$^{-1}$ K$^{-1}$ and $\hbar\nu_{ph} = 0.033$ eV) is shown by the dashed line.

$$A = \frac{1}{p^2 + q^2} \cdot \frac{p\sinh p + q\sin q}{\cosh p + \cos q} + \frac{\cosh p\cos q + 1}{(\cosh p + \cos q)^2}, \quad (16b)$$

where $p = \frac{2d}{\delta}\sqrt{\sqrt{1+\alpha^2} - \alpha}$, $q = \frac{2d}{\delta}\sqrt{\sqrt{1+\alpha^2} + \alpha}$, $\alpha = \varepsilon\omega/4\pi\sigma$, and $\delta = c/\sqrt{2\pi\sigma\omega}$.

The theoretical dependences of the parameters $D/A$, $D$, and $A$ of the Dysonian EPR lineshape (see Eq. (3)) on the $d/2\delta$ ratio at $\alpha \to 0$ and $d = 5 \cdot 10^{-5}$ m are shown in Fig. 12. Analysis showed that the calculated lineshape parameter $D/A$ is related to the experimental parameter $A/B$ (see Fig. 2) by the simple relationship $A/B = 1 + 1.45D/A$. This makes it possible to determine the *ac* conductivity of the polymer immediately from its EPR spectrum.

As in the preceding case, the specific conductivity of the PAn · $H_2SO_4$ specimen with the oxidation level $y = 0.53$ decreases as the temperature increases from a certain minimum value to the critical temperature $T_c \approx 190$ K; however, the specific conductivity again begins increasing on heating above $T_c$ (see Fig. 11). Such a dependence with an extremum can be explained assuming that several successive charge transfer processes proceed in the polymer. As in the case of PAn · $H_2SO_4$ with the oxidation level $y = 0.22$, the low-temperature branch of the dependence obtained can be interpreted in the framework of the model of scattering of charge carriers by the optical phonons of the PAn · ES(A) lattice. At high temperatures, the charge transfer described in the framework of the Mott model of interchain VRH of charge carriers can occur. The overall conductivity of this specimen can be expressed using the following relation:

$$\sigma_{ac} = \sigma_0^{(1)} + \left\{\left[\left(\sigma_0^{(2)}T\right)^{-1} + \left(\sigma_0^{(3)}T\right)^{-1}\left[\sinh\left(\frac{2\pi\hbar\nu_{ph}}{k_BT}\right) - 1\right]^{-1}\right]^{-1}\right\}^{-1}, \quad (17)$$

where the constants $\sigma_0^{(2)}$ and $\sigma_0^{(3)}$ are the corresponding constants from Eqs. (12b) and (15). As can be seen in Fig. 11, the temperature dependence for the PAn · $H_2SO_4$ specimen with the oxidation level $y = 0.53$ is well fitted using Eq. (17) with the parameters $\sigma_0^{(1)} = 6.8 \cdot 10^3$ S m$^{-1}$, $\sigma_0^{(2)} = 43.5$ S m$^{-1}$ K$^{-1}$, $\sigma_0^{(3)} = 6.9$ S m$^{-1}$ K$^{-1}$, and $2\pi\hbar\nu_{ph} = 0.047$ eV. The last-named value exceeds the energy of phonons in PAn · $H_2SO_4$ with $y = 0.22$, which indicates an increase in the crystallinity of the fully oxidized polymer. However, this value is also close to the activation energy of torsional vibrations of the polymer chains. This indicates a close relation between the molecular and electrodynamic processes in PAn · $H_2SO_4$. In particular, for this specimen we can calculate $\alpha = 6.5 \cdot 10^{11}$ eV m$^{-1}$ at $N = 2.0 \cdot 10^{27}$ m$^{-3}$. The calculated constant of the electron-phonon interaction in this specimen also much exceeds the corresponding value for *trans*-PAc. The *ac* conductivity of clusters in oxidized PAn · $H_2SO_4$ ($y = 0.53$) is ~1400 S m$^{-1}$ at room temperature (see Fig. 11), which is also much lower than the conductivity calculated for this specimen.[62]

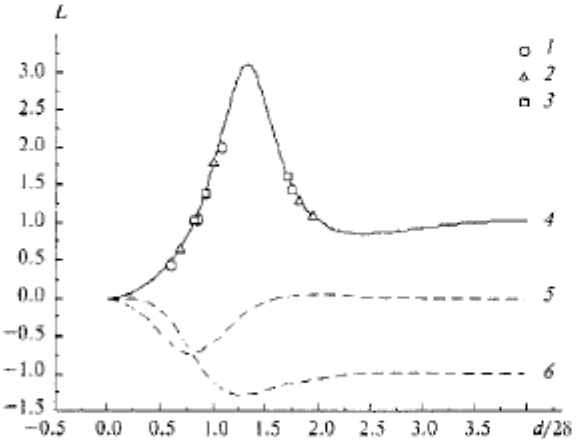


**Fig. 12.** Dependences of the asymmetry parameter $D/A$ (*1*—*3*) on the ratio $d/2\delta$ of the half-thickness of the specimen to the depth of the skin layer, calculated using Eqs. (3) and (16) for specimens of PAn · CS with $y = 0.5$ (*1*) and 0.6 (*2*) and for PAn · AMPS with $y = 0.6$ (*3*) and different thickness. Theoretical dependence of the asymmetry parameter $D/A$ (*4*) is shown by the solid line; those of the $A$ (*5*) and $D$ (*6*) components, calculated using Eqs. (3) and (16) at $\alpha \to 0$, are shown by dashed lines.

Thus, oxidation of PAn to $y \geq 0.03$ results in the increase in the number and size of highly conducting clusters with the highly mobile charge carriers, which is the reason for the Raman relaxation processes, as well as for the increase in the conductivity and in the Pauli magnetic susceptibility. An increase in the dimensionality of the system upon oxidation changes the mechanism of charge transport from isoenergetic interchain charge tunneling to interchain VRH of the charge carriers.

The concentration of diamagnetic charge carriers in PAn with the oxidation level in the range $0.22 \leq y < 0.5$ equals or is somewhat higher than the spin concentration. This means that the charge in these specimens is transferred by polarons mostly, whereas the charge in the fully doped ES(A) form of PAn is transferred by diamagnetic bipolarons. By and large the data obtained are in agreement with the concept of stabilization in PAn of metal-like clusters built of strongly interacting polymer chains with 3D-delocalized conduction electrons[60,61]; however, they don't confirm the theory completely.

Interaction between the charge carriers and the lattice phonons in PAn · $H_2SO_4$ is much stronger than in *trans*-PAc and other COP, which is likely due to the closer packing and greater planarity of the polymer chains in PAn · $H_2SO_4$. As a result, the charge transfer integral between the polymer chains is modulated by ultraslow librations of macromolecules, which manifests itself to the greatest extent in fully oxidized PAn.

### Polyaniline doped with hydrochloric acid

As in the case of PAn · $H_2SO_4$, the 3-cm wave band EPR spectrum of PC in PAn · HCl exhibits a symmetric singlet line (Fig. 13, *a*) whose width $\Delta B_{pp}$ for both the initial and weakly oxidized specimens is virtually independent of temperature. In the oxidized polymer with $y > 0.03$ the $\Delta B_{pp}$ value exhibits a bell-shaped temperature dependence with the inflection point at the critical temperature $T_c \approx 200$ K. The linewidth increases almost linearly at $T \leq T_c$ and decreases at higher temperatures.

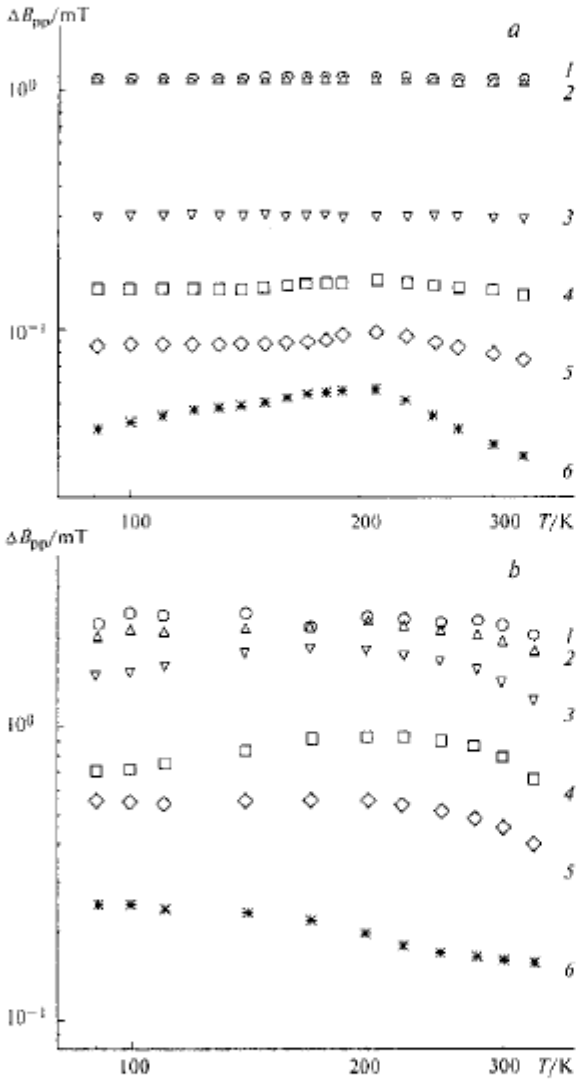


**Fig. 13.** Temperature dependences of the peak-to-peak width of the absorption line of paramagnetic centers in the initial specimen (*1*) and in the specimens of PAn · HCl with $y \approx 0.01$ (*2*), 0.03 (*3*), 0.22 (*4*), 0.41 (*5*), and 0.50 (*6*) in the 3-cm (*a*) and 2-mm (*b*) EPR wave bands.

The absorption spectrum of this polymer also exhibits a HFS (see Fig. 3). Unlike PAn · $H_2SO_4$, the HFI constants $a_i$ and spin densities $\rho_i$ calculated using the McConnel equation with coefficients of proportionality $Q$ equal to 2.25 and 2.37 mT for H and N atoms, respectively,[103,121] vary monotonically with the oxidation degree of the polymer (Table 1).

On going to the 2-mm wave band the $\Delta B_{pp}$ value becomes more sensitive to variations of the temperature and conductivity of the polymer (see Fig. 13, *b*).

Two types of PC are stabilized in PAn · HCl. These are $R_1$ with the magnetic parameters $g_{xx} = 2.00535$, $g_{yy} = 2.00415$, $g_{zz} = 2.00238$, $A_{xx} = A_{yy} = 0.33$ mT, and $A_{zz} = 2.3$ mT and $R_2$ with the magnetic parameters $g_\perp = 2.00351$ and $g_\parallel = 2.00212$. The relative content $n_1/(n_1 + n_2)$ of PC of the $R_1$ type varies as the temperature and degree of oxidation vary, much as it occurs in PAn · $H_2SO_4$ (see Fig. 5). This can be explained by the increase in the number of mobile spin charge carriers and by the formation of the polaron lattice in the oxidized polymer above the percolation threshold.

Using $A_{xx} = A_{yy} = 1.25$ mT for PC in pernigraniline[122] and the McConnel constant $Q = 2.25$ mT,[103] one can calculate the spin density $\rho_N(0)$ on the nucleus of the N atom, $\rho_N(0) = (A_{xx} + A_{yy} + A_{zz})/(3Q) = 0.65$. Then, using the components of the g-tensor (see above) and Eq. (1), we can calculate the energies of electron excitation to the nearest molecular orbitals ($\Delta E_{n\pi^*} = 4.0$ eV and $\Delta E_{\sigma\pi^*} = 6.6$ eV).

Since the averaged *g*-factors of radicals $R_1$ and $R_2$ are approximately equal, by applying Eq. (2) one can determine the minimum rate of diffusion of the polaron of the $R_2$ type along the polymer chain of the ES(A) form of PAn ($\nu_{1D}^0 \geq 10^9$ s$^{-1}$).

The conformation of the polymer chain and the spin density distribution affect the magnetic parameters of PAn · HCl. Taking into account that the spin transfer integral ($I_{C-N}$) between the $p_z$-orbitals of the C and N atoms depends on the dihedral angle in PAn as $I_{C-N} \propto \cos\theta$ and using the $\theta$ value for the EB form of PAn (56°),[107] we can determine from Eq. (1) that PAn · HCl with $y = 0.22$ is characterized by $\theta = 33°$ and $\rho_N^\pi = 0.42$. Hence it follows that the dihedral angle $\theta$ decreases on oxidation, thus increasing the $I_{C-N}$ integral and, therefore, the spin density on the benzene

**Table 1.** Dependence of the HFI constants ($a_i$/mT) and the spin density on the nuclei of H and N atoms ($\rho_i \cdot 10^{-2}$) on the degree of oxidation ($y$) of the PAn specimens

| $y$ | $a_H$ | $a_H^*$ | $a_N$ | $\rho_H$ | $\rho_H^*$ | $\rho_N$ |
|---|---|---|---|---|---|---|
| 0.00 | 0.41 | — | 0.14 | 182 | — | 59.1 |
| ~0.01 | 0.31 | — | 0.10 | 138 | — | 42.2 |
| ~0.03 | 0.28 | — | 0.092 | 124 | — | 38.8 |
| 0.22 | 0.024 | — | $7.6 \cdot 10^{-3}$ | 107 | — | 3.21 |
| 0.41 | 0.014 | — | $4.6 \cdot 10^{-3}$ | 6.22 | — | 1.94 |
| 0.50 | $5.3 \cdot 10^{-3}$ | $9.5 \cdot 10^{-4}$ | $1.8 \cdot 10^{-3}$ | 2.36 | 0.422 | 0.760 |

* The values obtained for the nucleus of the central H atom.

ring. The variation of the magnetic parameters is a consequence of both greater spin delocalization along the polymer chain and greater planarity of polymer chains during the oxidation of PAn.

The lineshape of radicals of the $R_2$ type changes appreciably on the percolation transition in PAn · HCl (in the range $0.03 \le y \le 0.22$). If at $y \ge 0.03$ and $T < 300$ K we have $g_\perp > g_\parallel$, then even at $y \ge 0.22$ the inequality $g_\perp < g_\parallel$ holds. Previously,[84] we observed an analogous effect in studies of the interaction of PAn with water vapor and explained it by appreciable change in the conformation of the microenvironment of radicals of the $R_2$ type caused by the formation of water bridges between the polymer chains. The above-mentioned change in the lineshape can also be explained by structural changes occurring on the percolation transition in PAn.

As in the case of PAn · $H_2SO_4$, the effects of rapid passage are observed in the 2-mm wave band EPR spectra of PAn · HCl if the conditions of adiabatic passage of resonance $\gamma_e\omega_m B_m \ll \gamma_e^2 B_1^2$ and spin packet saturation $\gamma_e B_1 \sqrt{T_{r1}T_{r2}} \ge 1$ hold. These effects were used for determining the relaxation and dynamic parameters of PC in these specimens. The $T_{r1}$ values vary on oxidation of the polymer as $T_{r1} \propto nT^l$, where $l = 3$—$4$ at $y < 0.03$ and $l = 0.3$ at $0.03 < y < 0.22$ (Fig. 14). This can be associated with intensification of the spin-spin exchange between the PC localized on neighboring polymer chains due to increase in the size and number of metal-like clusters on oxidation of PAn. Apart from this, such a change in the relaxation properties of PC indicates a drastic change in the rate of energy transfer from the spin ensemble to the polymer lattice as well as a change in the mechanism of charge transport during the oxidation of PAn.

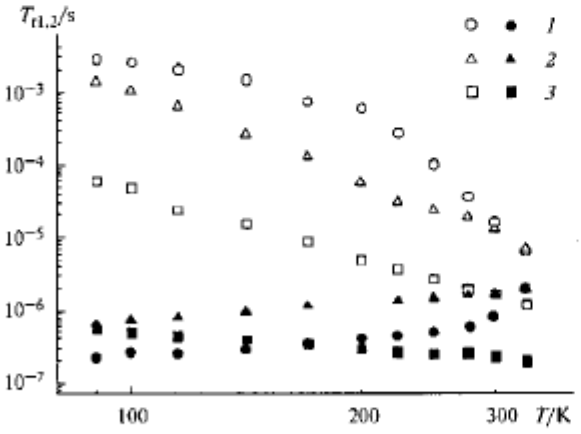


**Fig. 14.** Temperature dependences of the effective spin-lattice and spin-spin relaxation times ($T_{r1}$, open circles, and $T_{r2}$, filled circles, respectively) of paramagnetic centers in the initial specimen of PAn (*1*) and in specimens of PAn · HCl with $y \approx 0.01$ (*2*) and 0.03 (*3*).

The temperature dependence of the parameter $K_{mov} = u_3^x/u_3^y$ (see Fig. 7) was used for calculating the correlation time $\tau_c^x$ of the librations of the polymer chains carrying localized radicals of the $R_1$ type about the $x$ axis of the initial polymer, $\tau_c^x = 3.5 \cdot 10^{-5}\exp(0.015\ \text{eV}/(k_B T))$. Analogous dependence was also obtained for PAn · HCl with $y \approx 0.01$ and $y \approx 0.03$.

The temperature dependences of the coefficients of spin diffusion along and between the polymer chains ($D_{1D}$ and $D_{3D}$, respectively) are shown in Fig. 15. They were calculated using the procedure described above (Eqs. (9) and (10)) and from the data presented in Fig. 14 assuming spin delocalization over five monomer units of PAn.[118] From the data shown in Fig. 15 it follows that $D_{1D} \approx 10^{11}$ rad $s^{-1}$ and $D_{3D} \approx 10^8$ rad $s^{-1}$ at room temperature. The first value is more than two orders of magnitude lower than the rate of charge diffusion obtained previously for PAn with $y = 0.05$[66,70]; however, it is much higher than the calculated $\nu_\parallel^0$ value (see above). At $y \ge 0.22$, the times $T_{r1}$ and $T_{r2}$ become nearly equal due to the formation of metal-like clusters and to increase in the effective dimensionality of the system. In this case, the method of steady-state SHF saturation becomes less sensitive to the relaxation and dynamics of PC; however, the averaged effective spin diffusion coefficient can be assessed assuming that the spin motion along the polymer chain dominates and $2T_{r1} \cong T_{r2}$. This value is $D_{1D} = 1.6 \cdot 10^{12}$ rad $s^{-1}$, which is much smaller than that obtained previously by magnetic resonance methods in relatively weak magnetic fields.[66] From the data shown in Fig. 15 it follows that the $D_{1D}/D_{3D}$ ratio decreases as $y$ increases. This is additional evidence for the formation of bulky metal-like clusters and for increase in the crystallinity of oxidized PAn. In this case, the concentration of elec-

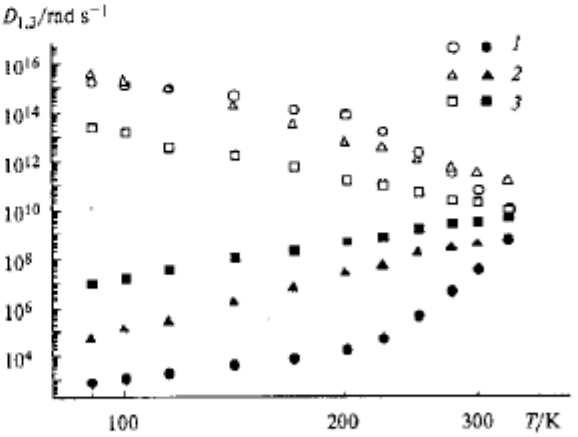


**Fig. 15.** Temperature dependences of the coefficients of diffusion of mobile paramagnetic centers along the polymer chains ($D_{1D}$, open circles) and between the polymer chains ($D_{3D}$, filled circles), calculated using Eqs. (9) and (10) for paramagnetic centers in the initial PAn specimen (1) and in specimens of PAn · HCl with $y \approx 0.01$ (2) and 0.03 (3).

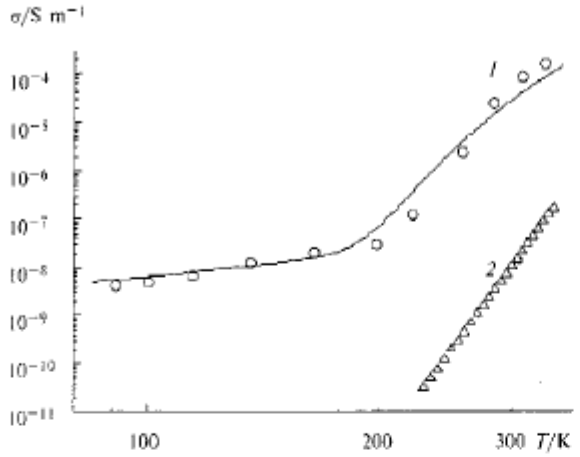


**Fig. 16.** Temperature dependences of the *ac* conductivity of the initial PAn specimen, calculated using Eq. (11) and the data shown in Fig. 15 (*1*), and of the *dc* conductivity (*2*). The overall *ac* conductivity, calculated using Eq. (18) with the parameters $\sigma_0 = 2.8 \cdot 10^{-6}$ S (m eV)$^{-1}$, $\hbar\nu_{ph} = 0.015$ eV, and $E_H = 0.042$ eV and using Eq. (19) with the parameters $\sigma_0 = 3.0 \cdot 10^4$ S eV m$^{-1}$, $E_H = 0.042$ eV, and $E_a = 0.397$ eV, is shown by the solid line.

tron traps and, hence, the probability of electron scattering by lattice phonons decrease, as is the case in inorganic amorphous semiconductors.[20]

Taking the diffusion coefficients of the spin and diamagnetic charge carriers to be equal and using Eq. (11), one can calculate $\sigma_{1D} = 10$ S m$^{-1}$ and $\sigma_{3D} = 1 \cdot 10^{-3}$—0.5 S m$^{-1}$ for the specimens with $0 < y < 0.03$ at room temperature. At $D_{1D} \geq D_{3D}$, these values are $\sigma_{1D} = (5—18) \cdot 10^3$ S m$^{-1}$ and $\sigma_{3D} = (3—10) \cdot 10^3$ S m$^{-1}$; as can be seen, the $\sigma_{3D}$ value increases more rapidly than the $\sigma_{1D}$ value on oxidation of the polymer, which is evidence for the increase in the number and dimensionality of metal-like clusters in PAn.

The plots of the temperature dependences of the *ac* conductivity calculated using Eq. (11) at $N = 9.5 \cdot 10^{23}$ m$^{-3}$ and $c_{1D} = 1.02$ nm[45] and those of the *dc* conductivity for the initial PAn specimen are shown in Fig. 16. The slope of the dependence $\sigma_{dc}(T) = 1.4 \cdot 10^{-62} T^{22}$ is nearly the same as that determined previously for PAn · EB,[123] at least at $T \geq T_c \approx 200$ K, and seems to be too steep to describe the charge transport in the framework of the Kivelson mechanism.[105] The $\sigma_{ac}(T)$ dependence presented has likely two branches with different temperature coefficients and has the inflection point at $T_c = 2\pi\hbar\nu_{ph}/k_B$ ($\nu_{ph}$ is the frequency of optical $2k_F$ phonons). This dependence can be interpreted in the framework of the short-polaron hopping model,[124] in which the polaron energy $E_H$ is dependent on distance, and at low temperatures ($T \leq T_c$) the $\sigma_{ac}(T)$ dependence is described by the formula

$$\sigma_{ac}(T) = \sigma_0 \left[ k_B T + \frac{4E_H}{\ln(2\nu_{ph}/\omega_c)} \ln\left(1 - \frac{k_B T}{E_H} \ln\frac{2\nu_{ph}}{\omega_c}\right)\right], \quad (18)$$

whereas at $T \geq T_c$ the hopping is dependent on both $E_H$ and the activation energies $E_a$, and the $\sigma_{ac}(T)$ dependence is given by the following formula:

$$\sigma_{ac}(T) = \frac{\sigma_0}{k_B T}\left(E_H/k_B T\right)^4 \exp\left(-\frac{E_a + E_H}{k_B T}\right). \quad (19)$$

The temperature dependence of the overall conductivity $\sigma_{ac}$ was calculated using Eq. (18) with the parameters $\sigma_0 = 2.8 \cdot 10^{-6}$ S (m eV)$^{-1}$, $2\pi\hbar\nu_{ph} = 0.015$ eV, and $E_H = 0.042$ eV and using Eq. (19) with the parameters $\sigma_0 = 3.0 \cdot 10^4$ S eV m$^{-1}$, $E_H = 0.042$ eV, and $E_a = 0.397$ eV (see Fig. 16). Good correlation of this dependence with the experimental data indicates that the parallel charge transfer by short mobile polarons occurs in the initial polymer. Previously,[123] analogous temperature dependences were observed for PAn · EB at relatively low recording frequencies and for lightly doped poly(tetrathiafulvalene) at different recording frequencies.[125,126]

As for other COP, the experimental data on the conductivity of weakly oxidized PAn specimens can be explained using the Kivelson model of isoenergetic charge transfer between nonlinear charge carriers.[25]

According to Eq. (14a), if the interpolaron charge transfer predominates, the $\sigma_{dc}(T)$ dependence should be of the form $\sigma_{dc}(T) \propto T^m$. It was actually observed for oxidized PAn · HCl specimens with $y \geq 0.01$ and 0.03 (Fig. 17).

The concentration of mobile spins ($y_p$) in PAn · HCl with $y \geq 0.01$ is $1.2 \cdot 10^{-4}$ per two benzene rings. Taking into account that each bipolaron carries the double elementary charge, we get $y_{bp} = 2.3 \cdot 10^{-3}$ and $\langle y \rangle = 4.6 \cdot 10^{-2}$. The concentration of anions, $N_i$, is $2.0 \cdot 10^{25}$ m$^{-3}$; therefore $R_0 = 2.28$ nm for this polymer. The constant $\gamma_0$ in Eqs. (14a) and (14b), determined from the slope of the $\sigma_{dc}(T)$ dependence, is equal to $3.5 \cdot 10^{19}$ s$^{-1}$. Assuming spin delocalization in the polaron over five monomer units[118] toward the principal $x$ axis of the polymer with the constant $c_{1D} = 1.02$ nm[45], we get $\xi_\parallel = 1.19$ nm. The perpendicular component $\xi_\perp$ of the quantity $\xi$ can be determined using the following equation[25]:

$$\xi_\perp = \frac{c_{3D}}{\ln(\Delta_0/t_\perp)}, \quad (20)$$

where $2\Delta_0$ is the band gap and $t_\perp$ is the component of the transfer integral, determined from the equation[127]

$$t_\perp = \frac{\hbar^4 D_{1D} \nu_{ph}^3}{2\pi E_p} \exp\left(\frac{2E_p}{\hbar\nu_{ph}}\right), \quad (21)$$

where $E_p$ is the formation energy of the polaron. The

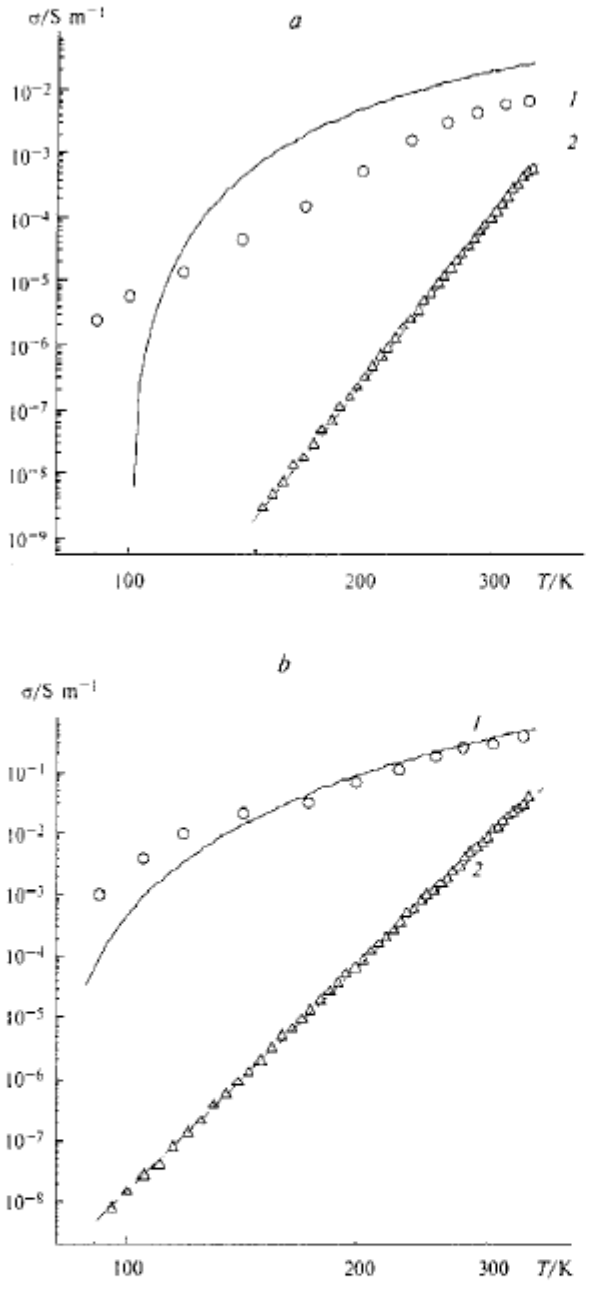


**Fig. 17.** Temperature dependences of the *ac* (*1*) and *dc* (*2*) conductivities calculated using Eq. (11) and the data presented in Fig. 15 for specimens of PAn · HCl with $y \approx 0.01$ (*a*) and 0.03 (*b*). The *ac* and *dc* conductivity calculated using Eq. (14) with the parameters $n = 15.2$, $\langle y \rangle = 0.046$, $\xi_\perp = 0.079$ nm, $\gamma_0 = 3.5 \cdot 10^{19}$ s$^{-1}$ (*a*), $n = 12.1$, $\langle y \rangle = 0.081$, $\xi_\perp = 0.087$ nm, $\gamma_0 = 2.1 \cdot 10^{17}$ s$^{-1}$ (*b*), $\xi_\parallel = 1.19$ nm, and $\nu_e = 140$ GHz are respectively shown by solid and dotted lines.

substitution of 3.8 eV[128] for $2\Delta_0$, 0.1 eV (this value is typical of $\pi$-conjugated polymers)[127] for $E_b$, $3.6 \cdot 10^8$ rad s$^{-1}$ (experimental value) for $D_{3D}$, and $3.6 \cdot 10^{12}$ s$^{-1}$ for $\nu_{ph}$ gives $t_\perp = 7.1 \cdot 10^{-3}$ eV, $\xi_\perp = 0.079$ nm, and $\xi = 0.2$ nm for PAn · HCl with $y \approx 0.01$. Analogous calculations for PAn · HCl with $y \approx 0.03$ and the parameters $y_p = 1.1 \cdot 10^{-3}$ and $y_{bp} = 1.2 \cdot 10^{-2}$ give $\langle y \rangle = 7.9 \cdot 10^{-2}$, $\gamma_0 = 2.1 \cdot 10^{17}$ s$^{-1}$, $\xi_\perp = 0.087$ nm, and $\xi = 0.21$ nm.

The temperature dependences of the *dc* conductivities of PAn · HCl specimens with degrees of oxidation $y \approx 0.01$ and $y \approx 0.03$ calculated using Eq. (14a) are respectively described by the equations $\sigma_{dc}(T) = 2.3 \cdot 10^{-42} T^{15.2}$ S m$^{-1}$ and $\sigma_{dc}(T) = 1.2 \cdot 10^{-32} T^{12.1}$ S m$^{-1}$ (see Fig. 17). Analysis of the $\sigma_{dc}(T)$ dependence (see Fig. 17, *a*) shows that a certain disagreement between the calculated and experimental data is observed for the PAn · HCl specimen with $y \approx 0.01$. Moreover, the $\gamma_0$ constant for this specimen is nearly two orders of magnitude larger than the corresponding value for *trans*-PAc ($\gamma_0 = 1.2 \cdot 10^{17}$ s$^{-1}$).[25] Better agreement between the experimental data and the Kivelson theory is observed for PAn · HCl with $y \approx 0.03$ (see Fig. 17, *b*), for which the $\gamma_0$ value virtually coincides with that for *trans*-PAc. This can be explained by an increase in the number and mobility of mobile charge carriers in the polymer with a higher degree of oxidation, which results in increase in the probability of hopping charge transfer between the polymer chains. Thus, the mechanism of charge transfer by short polarons is realized in the initial polymer. At the optimum degree of oxidation of the initial polymer, this mechanism changes to isoenergetic hopping of charge carriers between the polaron levels. At a lower degree of oxidation of the polymer, the charge transfer proceeds following both these mechanisms.

In the studies of the *dc* conductivity and thermoelectromotive force[39–42] it was suggested that 1D VRH charge transfer occurs in PAn · HCl specimens with different degrees of oxidation at low temperatures. It was established that the crystalline fraction of the polymer consists of clusters of strongly interacting oxidized polymer chains with 3D delocalized electrons between them. The 1D charge transfer occurring between such clusters likely makes the predominant contribution to the macroscopic *dc* conductivity of the polymer. It is likely that analogous electron transport processes also occur in the PAn · HCl specimens with $y \geq 0.22$ we studied along with the above-mentioned specimens.

From the plots shown in Fig. 18 it can be seen that the *dc* conductivity of the PAn · HCl specimens with $y \geq 0.22$ obeys fairly well the $T^{-1/2}$ law for 1D VRH charge transport (see Eq. (12a)). The percolation constants $T_0$, determined from the slopes of the corresponding dependences $\sigma_{dc}(T)$ (see Fig. 18), and average localization lengths $\langle L \rangle$ of charge carriers in these specimens, determined from the $n(\varepsilon_F)$ values, as well as the $L_\parallel$ and $L_\perp$ components of the quantity $\langle L \rangle$, determined using the method reported previously,[39] are presented in Table 2. The $\nu_0$ constant found for these polymers using

Eq. (12b) changes in the range $(3.4-4.8)\cdot10^{12}$ s$^{-1}$ and is close to that found for PAn · ES(A) $\nu_0 = 1.6\cdot10^{13}$ s$^{-1}$.[41] It should be noted that the frequency of lattice phonons $\nu_{ph} \approx k_B T_c/2\pi\hbar = 4.2\cdot10^{12}$ s$^{-1}$ is close to the above-listed $\nu_0$ value.

Oxidation of the polymer is accompanied by the formation of metal-like clusters with strong dipole-dipole interaction between the spin packets.

This results in an increase in the effective relaxation rate, which becomes higher than $\omega_m$. For this reason, the relaxation and dynamics of the clusters can hardly be studied by the method of steady-state SHF saturation. In this case, the above-mentioned method for analyzing the Dysonian lineshape can be used.

The temperature dependences of the *ac* conductivity of strongly oxidized PAn · HCl, determined from the 2-mm wave band EPR spectra using Eqs. (3) and (16) (Fig. 19), have a bell-like shape with a maximum value of $\sigma_{ac} = 1.1\cdot10^6$ S m$^{-1}$ near the critical temperature $T_c \approx 200$ K. This value of $\sigma_{ac}$ is about two orders of magnitude higher than the SHF conductivity obtained for PAn with $y = 0.50$ by conductometry at 6.5 GHz.[62] Such a dependence is additional evidence for 1D electron localization (the semiconductor mode) at $T \le T_c$ and for 3D charge delocalization (the metallic mode) at higher temperatures. The temperature dependences of the thermoelectromotive force $S$, $\sigma_{ac}$, and $D_{3D}$, obtained for a number of COP,[42,68,129–133] as well as the $T_{rl}(T)$, $D_{3D}(T)$, and $\Delta B_{pp}(T)$ dependences (see Figs. 13, *a*, 14, and 15) also have analogous shape and are characterized by a close $T_c$ value.

Analysis of the data showed that at low temperatures ($T \le T_c$) the $\sigma_{ac}(T)$ dependence obeys the Mott VRH law and can be described by Eq. (12b). At $T \ge T_c$, the conductivity becomes sensitive to interaction between the charge carriers and optical phonons of the lattice and is described by Eq. (15). In the framework of these mechanisms the theoretical temperature dependence of conductivity is described by the following equation:

$$\sigma_{ac} = \left\{\left(\sigma_0^{(2)}T\right)^{-1} + \left(\sigma_0^{(3)}T\right)^{-1}\left[\sinh\left(\frac{2\pi\hbar\nu_{ph}}{k_BT}\right) - 1\right]^{-1}\right\}^{-1}, \quad (22)$$

where the constants $\sigma_0^{(2)}$ and $\sigma_0^{(3)}$ are the corresponding constants of Eqs. (12b) and (15). As can be seen in the plots shown in Fig. 19, Eq. (22) with the parameters $\sigma_0^{(2)}$

**Table 2.** The percolation constant ($T_0$), spin concentration ($N$), density of states ($n(\varepsilon_F)$) near the Fermi level $\varepsilon_F$, and the average ($\langle L\rangle$), parallel ($L_\parallel$), and perpendicular ($L_\perp$) localization lengths of the wave function of the charge carrier in specimens of PAn

| $y$ | $N\cdot10^{25}$ /spin m$^{-3}$ | $T_0\cdot10^{-3}$ /K | $n(\varepsilon_F)$ /eV$^{-1}$ mol$^{-1}$ | $\langle L\rangle$ | $L_\parallel$ | $L_\perp$ |
|---|---|---|---|---|---|---|
| | | | | nm | | |
| 0.00 | 0.20 | — | — | — | — | — |
| ~0.01 | 0.37 | — | — | — | — | — |
| ~0.03 | 2.1 | — | — | — | — | — |
| 0.22 | 18 | 10.2 | 0.6 | 2.02 | 7.1 | 1.1 |
| 0.41 | 76 | 3.76 | 1.7 | 1.91 | 6.9 | 1.0 |
| 0.50 | 153 | 1.65 | 3.8 | 1.92 | 7.0 | 1.0 |

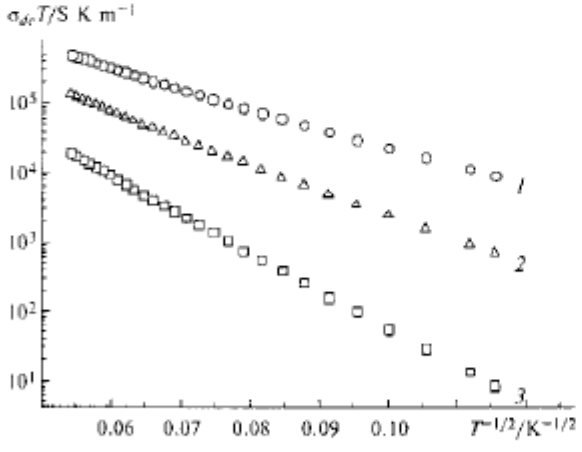


**Fig. 18.** Dependence of the product $\sigma_{dc}\cdot T$ on the quantity $T^{-1/2}$ for PAn · HCl with $y = 0.50$ (*1*), 0.41 (*2*), and 0.22 (*3*).

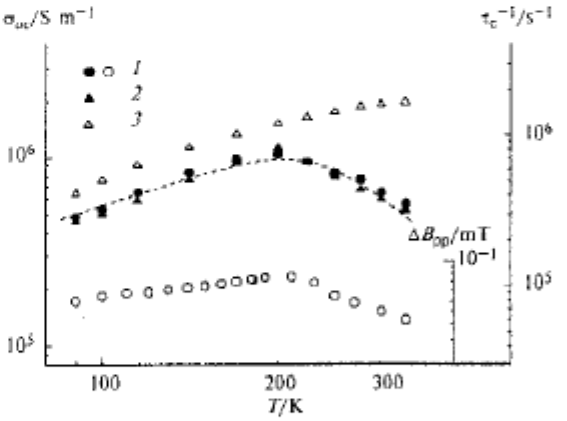


**Fig. 19.** Temperature dependences of the specific conductivity $\sigma_{ac}$ of specimens of PAn · HCl with oxidation levels $y = 0.41$ (*1*) and $y = 0.50$ (*2*) (filled circles), calculated from their EPR spectra and using Eqs. (3) and (16). The function calculated using Eq. (23) with the parameters $\sigma_0^{(2)} = 5.6\cdot10^3$ S m$^{-1}$ K$^{-1}$, $\sigma_0^{(3)} = 21.7$ S m$^{-1}$ K$^{-1}$, and $2\pi\hbar\nu_{ph} = 0.13$ eV is shown by the dashed line. The temperature dependence of the inverse correlation time of the polymer chain librations $\tau_c^{-1} = 2.9\cdot10^4\exp(-0.015\text{ eV}/(k_BT))$, calculated using Eq. (8) (*3*), and the temperature dependence of the linewidth $\Delta B_{pp}$ in a fully oxidized PAn · HCl specimen, presented in Fig. 13, *a* (*1*, open circles), are shown for comparison.

$= 5.6 \cdot 10^3$ S m$^{-1}$ K$^{-1}$, $\sigma_0^{(3)} = 21.7$ S m$^{-1}$ K$^{-1}$, and $2\pi\hbar\nu_{ph} = 0.13$ eV fits fairly good the temperature dependences for the specimens of PAn · HCl with oxidation levels $y = 0.50$ and $y = 0.41$. The phonon energy (0.13 eV) is higher than that obtained for PAn · $H_2SO_4$ with $y \geq 0.22$ and is evidence for higher crystallinity of PAn · HCl compared to PAn · $H_2SO_4$. As to the order of magnitude, it is also close to the activation energy of torsional vibrations of the polymer chains, which indicates a close relation between the molecular and electronic dynamic processes in PAn · HCl. In particular, the constant $\alpha$ for this specimen is $4.0 \cdot 10^{11}$ eV m$^{-1}$ at $N = 1.5 \cdot 10^{27}$ m$^{-3}$. The calculated constant of electron-phonon interaction in this specimen is somewhat smaller than the corresponding parameter for PAn · $H_2SO_4$; however, it is also much larger than the $\alpha$ value calculated for *trans*-PAc. The *ac* conductivity of clusters in fully oxidized PAn · HCl is higher than that of clusters in PAn · $H_2SO_4$; however, it is much lower than that calculated for PAn · ES(A).[62] The form of Eq. (22) indicates that two successive charge transfer processes proceed in the specimen.

Previously,[134] it was shown that the linewidth in the 3-cm wave band EPR spectrum of PAn · HCl and, hence, the rate of the spin-spin relaxation are proportional to the *dc* conductivity. Comparison of the plots of the $\sigma_{ac}(T)$ and $\Delta B_{pp}(T)$ functions shown in Fig. 19 confirms their additivity at least at $T \geq T_c$. It was also shown[135] that the rate of spin-spin relaxation is determined by the number of spins on each polymer chain ($N_S$) and by the number of neighboring chains ($N_c$) carrying the interacting spins.

$$T_{r2}^{-1} = \frac{4\left\langle \Delta\omega^2 \right\rangle}{5\nu_0 N_S}\left(21\ln\frac{\nu_n}{\nu_e} + 18\ln N_c\right) \qquad (23)$$

Using Eq. (23) with the parameters $T_{r2} = 1.7 \cdot 10^{-7}$ s, $\Sigma_{ij} = 1.2 \cdot 10^{51}$ m$^{-6}$, and $\nu_0 = 4.2 \cdot 10^{12}$ s$^{-1}$ (experimental value), a simple relation between these parameters can be obtained, $N_c \approx 55\exp(N_S)$. This means that at $L_\parallel = 7.0$ nm each polymer chain can carry up to seven interacting spins and that the spin packet of these PC can interact with $N_c = 20$ polymer chains. In this case the distance of 3D hops of both charge and spin carriers should meet the condition $3c_{3D} < L_\perp$.

Since the spin and charge transfer integrals can be modulated by the PAn lattice librations, the spin mobility and conductivity of PAn · HCl should also be dependent on the macromolecular dynamics, as is the case with other organic crystalline semiconductors.[136] It can be seen in Fig. 19 that, at least at $T \leq T_c$, the $\sigma_{ac}(T)$ dependence for metal-like clusters correlates with the function $1/\tau_c^N(T)$ of the polymer chain librations (see above). This indicates that the spin exchange and, hence, the charge transfer integral is modulated by torsional lattice motions. Since the moving polaron polarizes the electron and phonon states, one can suggest that the spin relaxation and charge transfer should be accompanied by scattering of charge carriers by the lattice phonons. Such cooperative processes involving charge carriers and phonons are likely the most important for 3D metal-like domains of strongly interacting chains of oxidized polymers.

The velocity of a charge carrier in fully oxidized polymer near the Fermi level is $v_F = 4c_\parallel/[\hbar n(\varepsilon_F)] = 2.5 \cdot 10^5$ m s$^{-1}$. This makes it possible to determine the interchain hopping frequency of the charge carrier $\nu_{1D} = v_F/L_\perp = 2.4 \cdot 10^{14}$ s$^{-1}$ and, hence (using Eq. (11)), the *ac* conductivity $\sigma_{ac} = 1.3 \cdot 10^6$ S cm$^{-1}$ at $L_\perp = 1.0$ nm (see Table 2) and $T_c \approx 200$ K. This $\sigma_{ac}$ value is close to that found for this specimen from analysis of its EPR spectra, which is an additional confirmation of the formation in PAn · HCl of metal-like clusters with 3D-delocalized electrons. Therefore, as in the case of classical metals, one can determine the effective mass $m^*$ of a charge carrier using the formula $m^* = (3\pi^2 N)^{1/3}\hbar v_F^{-1}$,[20] which is approximately equal to two electron masses. The free path length $l_i$ of the charge carrier, calculated using the formula $l_i = \sigma_{ac} m^* v_F/(Ne^2)$,[20] is ~8.0 nm at $T_c$, which is somewhat shorter than that of the soliton in *trans*-PAc.[32,137]

Thus, the charge transfer by short polarons occurs predominantly in the initial polymer, the probability of polaron hopping being strongly dependent on the energy of lattice phonons. Relatively narrow (compared to $k_BT$) distribution of the polaron energies in weakly oxidized PAn · HCl is a consequence of the predominance of the isoenergetic hopping charge transfer in this polymer. Therefore, both the $\sigma_{dc}(T)$ and $\sigma_{ac}(T)$ dependences for the optimally oxidized polymer can be described in the framework of the Kivelson model modified for COP with the polaron and bipolaron charge carriers, the latter being located near charged anions. This corresponds to the picture of intersoliton charge transfer in lightly doped (weakly oxidized) *trans*-PAc. The above-mentioned energy distribution is broadened and becomes wider than the energy $k_BT_c$ of lattice phonons on oxidation of PAn, therefore the VRH charge transfer should likely be dominant in this case.

An individual conducting chain becomes a center of crystallization on increase in the degree of oxidation, as well as on percolation transition, and bulky metal-like clusters are formed around such a center. This is accompanied by strengthening of the electron-phonon and interchain interactions and by increase in the degree of crystallinity of the polymer. Strengthening of interchain interaction plays an important role in stabilizing the metallic state in the polymer, where the 1D electron localization and the Peierls instability are leveled. The charge transfer in PAn is modulated by macromolecular librations of the polymer chains that form a metal-like cluster consisting of closely packed and interacting polymer chains sharing 3D delocalized electrons. This is in agreement with the theory of the formation of metal clusters in the amorphous phase of PAn; however, it contradicts the hypothesis for the existence of numerous isolated conducting chains in PAn · ES(A).

### Polyaniline doped with camphorsulfonic acid

The 3-cm wave band EPR spectra of PAn · CS with the oxidation level $y = 0.6$ recorded at different temperatures (Fig. 20) indicate that cooling of the films results in the narrowing of the overall spectrum and in change in its shape. The lines recorded at the effective $g$-factor ($g = 2.0028$) have Lorentzian shapes with the Dysonian component. The contribution of the dispersion signal to the EPR spectrum depends on the temperature and degree of oxidation of the polymer. The overall EPR spectrum is a superposition of individual lines of at least two types of paramagnetic centers ($R_1$ and $R_2$) with different magnetic and dynamic parameters. The spectra of each of these PC were calculated using Eqs. (3) and (16) by the method considered above. Figure 21 illustrates an example of calculations of the spectra of both types of radicals, whose overall spectrum is also compared here with the experimental spectrum of PAn · CS. The total concentration of PC in the specimens of PAn · CS with the oxidation level $y = 0.5$ and 0.6 is $3.1 \cdot 10^{26}$ and $2.6 \cdot 10^{26}$ m$^{-3}$, respectively. The ratio of the concentrations $[R_1]/[R_2]$ in these polymers is 1 : 118 and 1 : 136, respectively. The 8-mm wave band EPR spectrum of the specimen of PAn · CS with the oxidation level $y = 0.6$ (an asymmetric singlet line) is shown in Fig. 20 by a dashed line. This spectral pattern can be explained by appreciable broadening of the line of the $R_2$ radical due to increase in the recording frequency because of the difference in the $g$-factors of spin packets and, hence, by the decrease in their contribution to the overall EPR signal. Depending on the oxidation level of the polymer, the linewidth of radicals of the $R_1$ type increases by a factor lying in the range from 4 to 6 as the recording frequency increases.

The linewidth of radicals $R_1$ is virtually temperature-independent in the whole temperature range, whereas the linewidth of PC of the $R_2$ type is a nearly linear function of temperature with the inflection point at the critical point $T_c \approx 100$ K (Fig. 22). Analogous variations of the linewidth were observed in the studies of several organic metals based on radical ionic salts[2,138,139] and interpreted in the framework of the known model,[138] according to which molecular librations in low-dimensional metals can reduce the molecular symmetry and, thus, accelerate the scattering of the charge carriers moving along and between the stacks by the lattice phonons. The frequency of librations increases as the temperature decreases and/or the pressure increases; this should result in broadening of the EPR spectrum. In the framework of the above-mentioned theory the dependence of the linewidth on the scattering times of charge carriers moving along and between the principal molecular axes ($\tau_\parallel$ and $\tau_\perp$, respectively) are determined by the following relationship[138]:

$$\Delta B_{pp} = (\Delta g)^2 \left(a\tau_\parallel^{-1} + b\tau_\perp^{-1}\right), \qquad (24)$$

where $\Delta g$ is the difference between the $g$-factor and $g_e$; $\tau_\perp^{-1} = c|t_\perp|^2\tau_\parallel$, where $t_\perp$ is the integral of the charge carrier transfer between stacks; and $a$, $b$, and $c$ are constants.

The time $\tau_\parallel$ appreciably increases as the pressure increases, which affects the $b\tau_\perp^{-1}$ term of Eq. (24)[139] and results in broadening of the EPR spectrum. At the same time, a decrease in temperature strengthens the intrastack interaction (and time $\tau_\parallel$), which indirectly

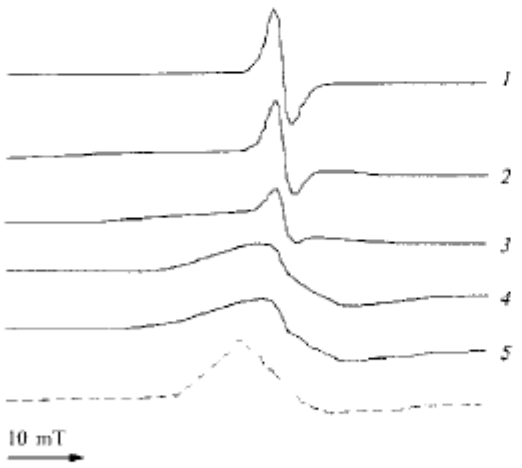


**Fig. 20.** 3-cm Wave band EPR spectra of PAn · CS with $y = 0.60$ at $T$/K = 9.5 (*1*), 51 (*2*), 95 (*3*), 210 (*4*), and 300 (*5*). The 8-mm wave band EPR spectrum of the same specimen at room temperature is shown by the dashed line.

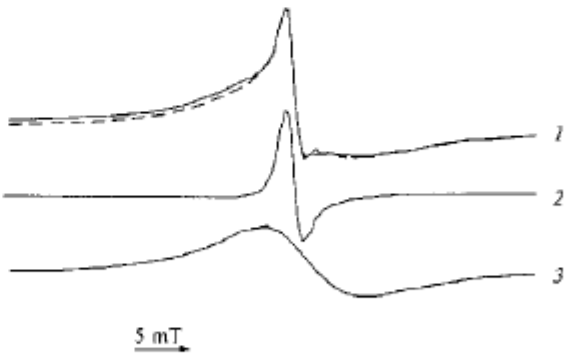


**Fig. 21.** 3-cm Wave band EPR spectrum of PAn · CS with $y = 0.6$ at 91 K (*1*, solid line) and the spectra of radicals $R_1$ (*2*) and $R_2$ (*3*), calculated using Eq. (3). The overall spectrum of radicals $R_1$ and $R_2$ is shown by the dashed line near spectrum (*1*).

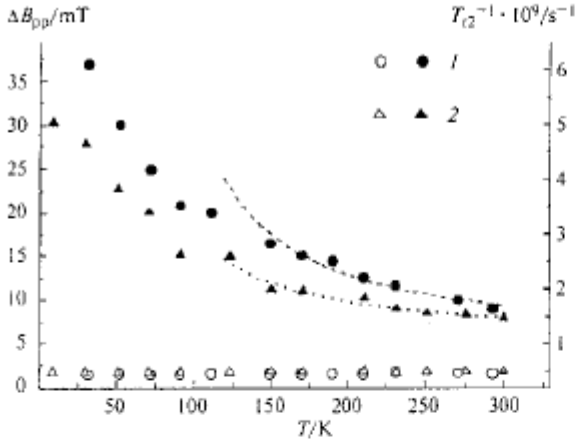


**Fig. 22.** Temperature dependences of the linewidth of paramagnetic centers $R_1$ (open circles and triangles) and $R_2$ (filled circles and triangles) in specimens of PAn · CS with $y = 0.50$ (*1*) and 0.60 (*2*). The functions $T_{r2}^{-1}(T) = 9.7 \cdot 10^8 \exp(0.015\ \text{eV}/k_B T)$ and $T_{r2}^{-1}(T) = 1.1 \cdot 10^9 \exp(0.010\ \text{eV}/k_B T)$ are shown by dotted and dashed lines, respectively.

affects the $\tau_\perp$ value. Therefore an increase in $\tau_\parallel$ due to the decrease in temperature and/or due to the increase in pressure eventually results in broadening of the EPR spectrum. Assuming that the interacting chains in the oxidized PAn · CS specimens form a crystalline phase, which is analogous to that in radical ionic salts, the above-mentioned phenomenological concept can also be applied to the specimens under study. The narrowing of the line on raising the PAn temperature can be explained by averaging of the local magnetic field caused by HFI between the localized spins whose energy levels lie near the Fermi level. The EPR line of PAn · CS may also be broadened to some extent by relaxation due to the spin-orbital interaction responsible for the linear dependence of $T_{r1}^{-1}$ on temperature[140]; however, this interaction seems to be rather weak in our case. It is significant that for both types of PC the linewidths are appreciably larger than those obtained previously for the fully oxidized powder-like and film-like PAn · CS (0.035 and 0.08 mT, respectively),[140] which indicates a higher conductivity of the specimens under study. Comparison of the $\Delta B_{pp}$ values for different PAn · CS specimens[91] suggested that a crystalline phase is formed in the amorphous phase of the polymer, beginning with the oxidation level $y = 0.3$, and that the paramagnetic centers of this newly formed phase exhibit a broader EPR spectrum. In the amorphous phase of the polymer, the paramagnetic centers of radicals of the $R_1$ type are characterized by nearly temperature-independent linewidth and are likely not involved in the charge transfer. At the same time, the magnetic resonance parameters of radicals of the $R_2$ type must reflect the electron transport in the crystalline domains of PAn · CS. Confirmation of this assumption requires analysis of the temperature dependence of paramagnetic susceptibility for both types of PC.

SHF-Radiation penetrates highly conducting compounds to only the depth of the skin layer. Therefore, only PC within this layer can be detected by EPR spectroscopy. Hence, the depth of the skin layer and its variation with temperature should be taken into account in order to determine the temperature dependence of the spin susceptibility. In the general case, the paramagnetic susceptibility $\chi_t$ can also contain a temperature-independent contribution $\chi_P$ due to the Pauli spins and a contribution $\chi_C$, which is due to localized spins and depends on the Curie temperature

$$\chi_t = \chi_P + \chi_C = 2\mu_B^2 n(\varepsilon_F) + \frac{Ng^2\mu_B^2}{4k_B T}. \qquad (25)$$

As can be seen in Fig. 23, the Curie susceptibility makes the predominant contribution to the paramagnetic susceptibility of PC of the $R_1$ radicals for both specimens in the whole temperature range. The susceptibility of the $R_2$ radicals also exhibits a similar dependence at $T < 100$ K. At higher temperatures, the Pauli susceptibility characteristic of classical metals[20] makes the main contribution to the $\chi_t$ value of the $R_2$ radicals in PAn · CS with the oxidation level $y = 0.60$. This makes it possible to determine the density of states near the Fermi level $n(\varepsilon_F)$ for the charge carriers, which is approximately equal to 1.2 $\text{eV}^{-1}$ per two phenyl rings and is in agreement with the value obtained previously in the optical (0.06–6 eV)[50] and EPR[140] studies of this polymer. Hence, one can calculate the Fermi energy of the Pauli $N$-spins using the equation[20] $\varepsilon_F = 3N/2n(\varepsilon_F) \approx 0.2$ eV at $N = 2.6 \cdot 10^{26}$ $\text{m}^{-3}$. This value is lower than the Fermi energy obtained for PAn · CS by the optical method (0.4 eV).[141] Assuming that the charge carrier mass is equal to the mass of a free electron ($m_c = m_e$), one can determine the number of charge carriers in such a quasimetal,[20] $N_c = (2m_c\varepsilon_F/\hbar^2)^{3/2}/3\pi^2 \approx 4.1 \cdot 10^{26}$ $\text{m}^{-3}$. This is close to the spin concentration in this polymer; therefore, one can conclude that all delocalized PC are involved in the charge transfer in PAn · CS with the oxidation level $y = 0.60$. The velocity of charge carriers near the Fermi level is[20] $v_F = 2c_{1D}/[\pi\hbar n(\varepsilon_F)] = 5.8 \cdot 10^5$ m $\text{s}^{-1}$ at $c_{1D} = 0.72$ nm[50] (this value is typical of COP[79,82]).

The paramagnetic susceptibility of PC of the $R_2$ radicals in oxidized PAn · CS ($y = 0.50$) exhibits a bell-shaped dependence of $\chi_2^{-1}$ on temperature (Fig. 23). As in the case of PAn doped with ammonia,[142] this should indicate a strong antiferromagnetic interaction of the spins due to the equilibrium between the triplet and singlet states in the system. Therefore, the last term in Eq. (25) can be written as[142]

$$\chi_C = \frac{N_C g^2\mu_B^2}{4k_B(T + \Theta)} + \frac{N_{T\Delta} g^2\mu_B^2}{k_B T} \cdot \frac{\exp(-J/k_B T)}{1 + 3\exp(-J/k_B T)}, \qquad (26)$$

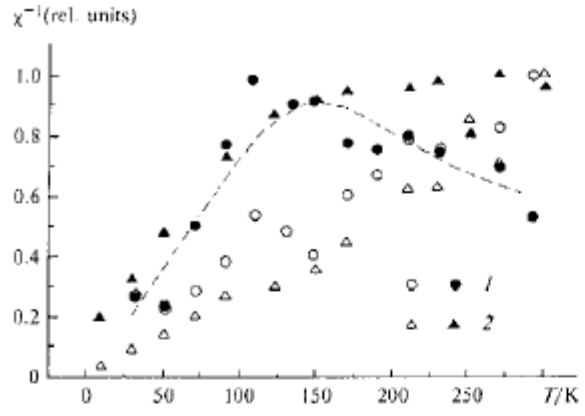


**Fig. 23.** Temperature dependences of the reduced inverse paramagnetic susceptibility of paramagnetic centers of the $R_1$ (open circles) and $R_2$ (filled circles) types in specimens of PAn · CS with $y = 0.50$ (*1*) and 0.60 (*2*). The temperature dependence calculated using Eq. (26) with the parameters $N_C/N_{TA} = 1/45$, $\theta = 5.5$ K, and $J = 0.072$ eV is shown by the dashed line.

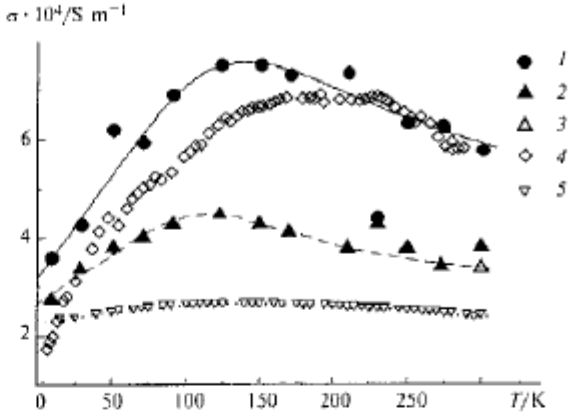


**Fig. 24.** Temperature dependences of the *ac* conductivity (*1* and *2*), calculated using Eqs. (3) and (16) from the 3-cm wave band EPR spectra of paramagnetic centers of the $R_1$ (*1*) and $R_2$ (*2*) types, and that of the *dc* conductivity (*5*) for a specimen of PAn · CS with $y = 0.60$. The *ac* conductivity (*3*) of the same specimen, determined from the 8-mm wave band EPR spectrum recorded at room temperature (see Fig. 20), and the temperature dependence of the *ac* conductivity of PAn · CS (*4*), determined by SHF conductometry at 6.5 GHz,[146] are shown for comparison. The functions $\sigma_{ac}(T)$ calculated using Eq. (17) with the parameters $\sigma_0^{(1)} = 3.2 \cdot 10^4$ S m$^{-1}$, $\sigma_0^{(2)} = 420$ S m$^{-1}$ K$^{-1}$, and $\sigma_0^{(3)} = 28$ S m$^{-1}$ K$^{-1}$ and with the parameters $\sigma_0^{(1)} = 2.7 \cdot 10^4$ S m$^{-1}$, $\sigma_0^{(2)} = 203$ S m$^{-1}$ K$^{-1}$, $\sigma_0^{(3)} = 6.1$ S m$^{-1}$ K$^{-1}$, and $2\pi\hbar\nu_{ph} = 0.047$ eV are shown by solid and dashed lines, respectively. The $\sigma_{dc}(T)$ dependence calculated using Eq. (27) with $\sigma_0^{(1)} = 2.3 \cdot 10^6$ S m$^{-1}$, $\sigma_0^{(2)} = 2.0 \cdot 10^5$ S m$^{-1}$ K$^{1/2}$, $\sigma_0^{(3)} = 6.7 \cdot 10^{-2}$ S m$^{-1}$ K$^{-1}$, $T_0 = 296$ K, and $2\pi\hbar\nu_{pin} = 0.13$ eV is shown by a dotted line.

where $N_C$ and $N_{TA}$ are the concentrations of the Curie spins and thermally activated spins, respectively, $\theta$ is a constant, and $J$ is the energy of the spin-spin interaction. As can be seen in Fig. 23, Eq. (26) with the parameters $N_C/N_{TA} = 1/45$, $\theta = 5.5$ K, and $J = 0.072$ eV fits fairly well the behavior of the paramagnetic susceptibility of oxidized PAn · CS with $y = 0.50$. The $J$ value (0.072 eV) is close to the corresponding energy (0.078 eV) obtained for PAn doped with ammonia.[142]

Thus, the charge carriers in the specimens of strongly oxidized PAn · CS are localized at temperatures below the critical temperature $T_c \cong 110$ K. This is the reason for VRH charge transfer between the polymer chains and for the Curie type of susceptibility of the specimen. At higher temperatures, when the energy of phonons becomes comparable with the value $k_B T_c = k_B T \approx 0.01$ eV, the charge carriers are scattered by the lattice phonons, which must affect the behavior of the high-temperature branch of the $T_{r2}(T)$ dependence. In fact, Fig. 22 shows that the functions $T_{r2}^{-1}(T) = 9.7 \cdot 10^8 \exp(0.015 \text{ eV}/k_B T)$ and $T_{r2}^{-1}(T) = 1.1 \cdot 10^9 \exp(0.010 \text{ eV}/k_B T)$ fit fairly well the high-temperature branches of the dependences $\Delta B_{pp}(T) \propto T_{r2}^{-1}(T)$ for radicals of the $R_2$ type in specimens of PAn · CS with the oxidation levels $y = 0.50$ and 0.60, respectively. The data presented show intensification of the spin-spin exchange at $T > T_c$, which is likely due to the activation librations of the polymer chains. The activation energies of these librations lie within the energy range characteristic of PAn · CS,[143] PAn · HCl,[86,88] and poly(tetrathiafulvalenes).[82,144,126] The $E_a$ value depends on the effective rigidity and planarity of the polymer chains that are eventually responsible for the electrodynamic properties of the polymer.

The $\sigma_{ac}(T)$ dependences obtained from the spectra of radicals of the $R_1$ and $R_2$ types in a specimen of oxidized PAn · CS with $y = 0.60$ have extrema (inflection points) at $T_c \cong 140$ K and 110 K, respectively (Fig. 24), and can also be described in the framework of VRH interchain charge transfer[29] at low temperatures and in the framework of the theory of charge carrier scattering by lattice phonons[32,119] at high temperatures. As can be seen in Fig. 24, the functions $\sigma_{ac}(T)$ calculated using the relationship $2\pi\hbar\nu_{ph} = 0.047$ eV and Eq. (17) with the parameters $\sigma_0^{(1)} = 3.2 \cdot 10^4$ S m$^{-1}$, $\sigma_0^{(2)} = 420$ S m$^{-1}$ K$^{-1}$, and $\sigma_0^{(3)} = 28$ S m$^{-1}$ K$^{-1}$ for radicals $R_1$ and $\sigma_0^{(1)} = 2.7 \cdot 10^4$ S m$^{-1}$, $\sigma_0^{(2)} = 203$ S m$^{-1}$ K$^{-1}$, and $\sigma_0^{(3)} = 6.1$ S m$^{-1}$ K$^{-1}$ for radicals $R_2$ are in good agreement with the experimental data. The values of the conductivities calculated from the 3-cm and 8-mm wave band EPR spectra of radicals $R_2$ are close. This means that, at least at high temperatures, the *ac* conductivity of the specimen depends only slightly on the EPR recording frequency, which is typical of conventional metals.[20] The maximum values

of the *ac* conductivity at $T_c$, calculated from the spectra of radicals $R_1$ and $R_2$, are $\sigma_{ac} \cong 7.6 \cdot 10^4$ and $\sigma_{ac} \cong 4.5 \cdot 10^4$ S m$^{-1}$, respectively. It appeared to be unexpected that the radicals of the $R_1$ type are more "sensitive" to variations of the conductivity and temperature of the specimen than the radicals of the $R_2$ type, whereas quite the reverse picture could be expected taking into account the location of these radicals in the polymer domains with different crystallinity. One of the reasons for such inconsistency can be their uniform and equiprobable distribution in the skin layer with an effective (averaged) conductivity, which can equally affect the shape of their EPR spectra. Since the localized radical has a narrower line, its spectrum should likely be more sensitive to the effective charge transfer in the polymer. The $\sigma_{ac}(T)$ dependence with a somewhat flattened extremum near $T_c \cong 200$ K, obtained for PAn · CS by SHF conductometry at 6.5 GHz,[144] is also shown for comparison in Fig. 24.

In the framework of the above-mentioned mechanisms of charge transfer the overall *dc* conductivity of the specimen is described by the following relationship (see Eqs (12a) and (15)):

$$\sigma_{dc} = \sigma_0^{(1)} + \left\{\left(\sigma_0^{(2)}T^{-1/2}\right)^{-1}\exp\left[-\left(\frac{T_0}{T}\right)^{1/2}\right] + \left(\sigma_0^{(3)}T\right)^{-1}\left[\sinh\left(\frac{2\pi\hbar\nu_{ph}}{k_BT}\right) - 1\right]^{-1}\right\}^{-1}. \quad (27)$$

As can be seen from Fig. 24, the $\sigma_{dc}(T)$ functions calculated using Eq. (27) with the parameters $\sigma_0^{(1)} = 2.3 \cdot 10^4$ S m$^{-1}$, $\sigma_0^{(2)} = 2.0 \cdot 10^5$ S m$^{-1}$ K$^{1/2}$, $\sigma_0^{(3)} = 6.7 \cdot 10^{-2}$ S m$^{-1}$ K$^{-1}$, $T_0 = 296$ K, and $2\pi\hbar\nu_{ph} = 0.13$ eV correlate well with the experiment. The phonon frequency $\nu_{ph} = 3.1 \cdot 10^{13}$ s$^{-1}$ is close to $\nu_0 = 1.6 \cdot 10^{13}$ s$^{-1}$ and to the corresponding frequency reported for PAn · HCl.[41] The average localization length $\langle L \rangle$ of the charge carrier is 6.2 nm, which is somewhat longer then the corresponding value calculated for PAn · CS (2.2—5.5 nm).[54]

Thus, both localized and mobile PC ($R_1$ and $R_2$, respectively) are formed simultaneously on oxidation in different domains of the PAn · CS specimens. At temperatures below 100 K, this results in the appearance of temperature-dependent Curie spin susceptibility characteristic of localized unpaired spins, whereas at higher temperatures this gives rise to the temperature-independent Pauli susceptibility, which is characteristic of the spins in metals. A rather strong antiferromagnetic interaction due to the singlet-triplet equilibrium is observed in oxidized PAn · CS with $y = 0.50$. The hypothesis for the absence of paramagnetism in PAn · CS with highly ordered and uniformly distributed anions, which is characteristic of an ideal bipolaron system, contradicts our experimental data. Analysis of the *ac* and *dc* conductivities showed that PAn · CS possesses better (compared to PAn · $H_2SO_4$ and PAn · HCl) electrodynamic properties characteristic of metals. The temperature at which the mode of the behavior of the $\chi(T)$ function changes from the Curie to the Pauli type roughly approximates that at which the transition occurs from the positive to the negative temperature coefficient of the *dc* conductivity of this polymer (see Figs. 23 and 24). Thus, PAn · CS is a disordered metal with the critical mode of the metal—insulator transition. The Curie contribution to the paramagnetic susceptibility decreases as the oxidation level increases to the optimum value $y = 0.60$; this is accompanied by increase in the PAn · CS crystallinity. Since this correlates well with the electron transport process, one can conclude that PC of the $R_2$ radicals stabilized in the crystalline domains of the specimen participate in the electron transport, whereas PC of the $R_1$ radicals localized in the amorphous domain of the polymer are involved in this process only indirectly. The crystalline clusters of the polymer are quasimetallic aggregates with strongly interacting polymer chains and 3D delocalized generalized charge carriers. The charge transfer between such clusters occurs jumpwise through amorphous domains characterized by lower mobility of the spin and charge carriers.

### Polyaniline doped with 2-acrylamido-2-methyl-1-propanesulfonic acid

Oxidized PAn · AMPS and PAn · CS specimens exhibit doublet 3-cm wave band EPR spectra with an effective *g*-factor ($g = 2.0020$), Lorentzian lineshape, and Dysonian components. Individual lines were assigned to PC of the $R_1$ and $R_2$ types, located in the amorphous and crystalline phase of the polymer, respectively. The overall concentration of PC in PAn · AMPS specimens with the oxidation levels $y = 0.4$ and 0.6 is $4.1 \cdot 10^{25}$ and $3.2 \cdot 10^{27}$ m$^{-3}$, respectively. The ratio of the concentrations $[R_1]/[R_2]$ in these specimens is 1 : 30 and 1 : 52, respectively, which is much lower than that determined for PAn · CS. On going to the 8-mm wave band the spectra of PAn · AMPS are also transformed into singlet Lorentzian lines with Dysonian components and linewidths $\Delta B_{pp}$ of 3.52 and 1.70 mT, respectively. This spectrum was also assigned to radicals $R_1$.

As in the case of PAn · CS, the linewidth of radicals $R_1$ in PAn · AMPS is virtually independent of temperature, whereas that of radicals $R_2$ monotonically changes with temperature. At $T \geq T_c \cong 120$ K, it can be approximated by the function $T_{r2}^{-1}(T) = 1.0 \cdot 10^9\exp(0.0052\ \text{eV}/k_BT)$ for the specimen with the degree of oxidation $y = 0.40$ and by the function $T_{r2}^{-1}(T) = 8.1 \cdot 10^8\exp(0.0078\ \text{eV}/k_BT)$ for the specimen with $y = 0.60$ (Fig. 25). The activation energies of the PC are about half as high as

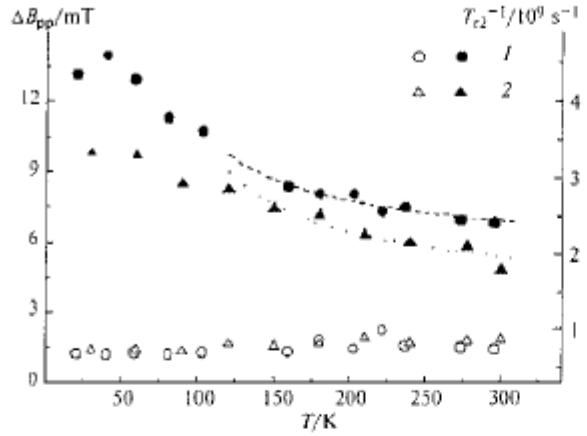


**Fig. 25.** Temperature dependences of the linewidth of paramagnetic centers of the $R_1$ (open circles) and $R_2$ (filled circles) types in the specimens of PAn · AMPS with $y = 0.40$ (*1*) and 0.60 (*2*). The functions $T_{r2}^{-1}(T) = 1.0 \cdot 10^9 \exp(0.0052\ \text{eV}/k_BT)$ and $T_{r2}^{-1}(T) = 8.1 \cdot 10^8 \exp(0.0078\ \text{eV}/k_BT)$ are shown by dashed and dotted lines, respectively.

the corresponding values for PAn · CS and the activation energies of the polymer chain librations in PAn · CS,[143] PAn · HCl,[86,88] and poly(tetrathiafulvalenes).[82,113,126] Such a difference may indicate a greater planarity and closer packing of the polymer chains in PAn · CS compared to PAn · AMPS. The linewidth of PAn appreciably decreases on replacement of the CS anion by the AMPS anion (see Figs. 22 and 25), which is likely due to the shortening of $\tau_1$ in Eq. (24). In addition, the number of mobile PC in the polymer decreases on such replacement, which can affect the conductivity of these polymers.

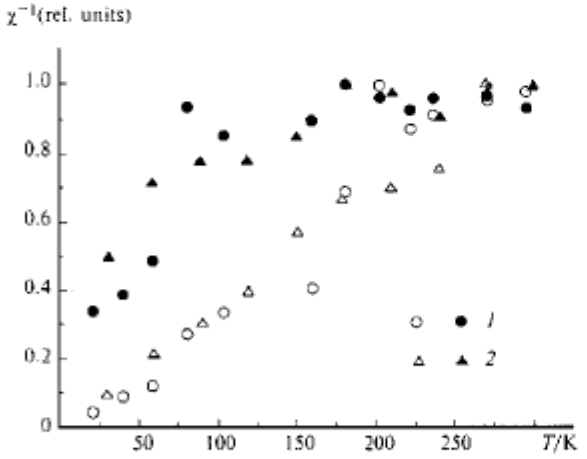


**Fig. 26.** Temperature dependences of the reduced inverse paramagnetic susceptibility of paramagnetic centers of the $R_1$ (open circles) and $R_2$ (filled circles) types in the specimens of PAn · AMPS with $y = 0.40$ (*1*) and 0.60 (*2*).

As in the case of PAn · CS, the Curie susceptibility $\chi_C$ makes the major contribution to the $\chi_c$ value of PC of the $R_1$ type (see Eq. (25)). At $T \geq T_c \approx 100$–120 K, this also holds for the susceptibility of PC of the $R_2$ type (Fig. 26). At high temperatures, the magnetic properties of the $R_2$ radicals are mainly determined by the first term of Eq. (25), which indicates delocalization of these PC and manifestation of metallic properties of the polymer in this temperature range.

Thus, the charge carriers in oxidized PAn · AMPS specimens are localized at $T \leq T_c$ and their transfer between the polymer chains can occur in the framework of the Mott VRH mechanism.[29] At $k_BT \geq k_BT_c \approx 0.009$ eV, the charge carriers in the polymer can be scattered by the lattice phonons, as is the case with PAn · CS.

As for PAn · CS, the $\sigma_{ac}(T)$ dependences for the PAn · AMPS specimen (Fig. 27), with extrema (inflection points) at $T_c \approx 220$ K and 150 K for the $R_1$ and $R_2$ radicals, respectively, can also be described in the framework of interchain VRH charge transfer[29] at low temperatures and in the framework of the theory of scattering of charge carriers by the lattice phonons[32,119] at $T \geq T_c$. As can be seen in Fig. 27, the $\sigma_{ac}(T)$ functions calculated using Eq. (17) with the

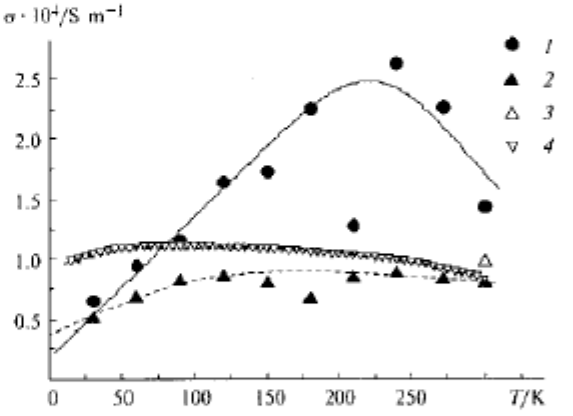


**Fig. 27.** Temperature dependences of the *ac* conductivity (*1* and *2*), calculated using Eqs. (30) and (16) from the 3-cm wave band EPR spectra of paramagnetic centers of the $R_1$ (*1*) and $R_2$ (*2*) types, and that of the *dc* conductivity (*4*) for the specimen of PAn · AMPS with $y = 0.60$. The *ac* conductivity (*3*) of the same specimen, determined from the 8-mm wave band EPR spectrum recorded at room temperature, is shown for comparison. The functions $\sigma_{ac}(T)$ calculated using Eq. (17) with the parameters $\sigma_0^{(1)} = 1.8 \cdot 10^3$ S m$^{-1}$, $\sigma_0^{(2)} = 118$ S m$^{-1}$ K$^{-1}$, $\sigma_0^{(3)} = 0.15$ S m$^{-1}$ K$^{-1}$, and $2\pi\hbar\nu_{ph} = 0.166$ eV and with the parameters $\sigma_0^{(1)} = 3.9 \cdot 10^3$ S m$^{-1}$, $\sigma_0^{(2)} = 46.7$ S m$^{-1}$ K$^{-1}$, $\sigma_0^{(3)} = 11.7$ S m$^{-1}$ K$^{-1}$, and $2\pi\hbar\nu_{ph} = 0.031$ eV are shown by solid and dashed lines, respectively. The $\sigma_{dc}(T)$ dependence calculated using Eq. (27) with $\sigma_0^{(1)} = 6.7 \cdot 10^3$ S m$^{-1}$, $\sigma_0^{(2)} = 1.0 \cdot 10^5$ S m$^{-1}$ K$^{1/2}$, $\sigma_0^{(3)} = 1.8 \cdot 10^{-3}$ S m$^{-1}$ K$^{-1}$, $T_0 = 72.4$ K, and $2\pi\hbar\nu_{ph} = 0.23$ eV is shown by the dotted line.

parameters $\sigma_0^{(1)} = 1.8 \cdot 10^3$ S m$^{-1}$, $\sigma_0^{(2)} = 118$ S m$^{-1}$ K$^{-1}$, $\sigma_0^{(3)} = 0.15$ S m$^{-1}$ K$^{-1}$, and $2\pi\hbar\nu_{ph} = 0.166$ eV for the $R_1$ radicals and with the parameters $\sigma_0^{(1)} = 3.9 \cdot 10^3$ S m$^{-1}$, $\sigma_0^{(2)} = 46.7$ S m$^{-1}$ K$^{-1}$, $\sigma_0^{(3)} = 11.7$ S m$^{-1}$ K$^{-1}$, and $2\pi\hbar\nu_{ph} = 0.031$ eV for the $R_2$ radicals are in good agreement with the experimental $\sigma_{ac}(T)$ dependences. At least in the high-temperature range the *ac* conductivity of the polymer, due to delocalized $R_2$ radicals, depends only slightly on the recording frequency (see Fig. 27), which is typical of conventional metals.[20] The maximum *ac* conductivity at $T_c$, calculated from the spectra of radicals $R_1$ and $R_2$, is, respectively, $\sigma_{ac} \cong 2.6 \cdot 10^4$ and $\sigma_{ac} \cong 8.8 \cdot 10^3$ S m$^{-1}$, which are much lower than the corresponding values for PAn · CS (see Fig. 24). This confirms the above-mentioned hypothesis for better electrodynamic characteristics of PAn · CS compared to PAn · AMPS because of the greater planarity and closer packing of the chains of the former. The plot of the temperature dependence of the *dc* conductivity of this specimen[145] is also shown in Fig. 27. As can be seen, the $\sigma_{dc}(T)$ functions calculated in the framework of the above-mentioned mechanisms using Eq. (27) with the parameters $\sigma_0^{(1)} = 6.7 \cdot 10^3$ S m$^{-1}$, $\sigma_0^{(2)} = 1.0 \cdot 10^5$ S m$^{-1}$ K$^{1/2}$, $\sigma_0^{(3)} = 1.8 \cdot 10^{-3}$ S m$^{-1}$ K$^{-1}$, $T_0 = 72.4$ K, and $2\pi\hbar\nu_{ph} = 0.23$ eV fit well the experimental data. The frequency of the lattice phonons $\nu_{ph} = 5.5 \cdot 10^{13}$ s$^{-1}$ in this polymer is somewhat higher than those in PAn · CS and other COP.[41] In particular, we can calculate $\alpha = 4.4 \cdot 10^{13}$ eV m$^{-1}$ at $N = 3.2 \cdot 10^{27}$ m$^{-6}$ for this specimen. The calculated constant of the electron-phonon interaction in PAn · CS is appreciably larger than the corresponding values for *trans*-PAc,[32] PAn · $H_2SO_4$, and PAn · HCl.

Thus, the localized and mobile PC ($R_1$ and $R_2$, respectively) are formed on oxidation of PAn · AMPS, as is the case with other PAn · ES(A). At low temperatures, the polymer exhibits Curie paramagnetism due to the localized PC. At high temperatures, PAn · AMPS exhibits the Pauli paramagnetism characteristic of delocalized spins in classical metals.

Analysis showed that PAn · AMPS possesses better electronic properties characteristic of metals than PAn · $H_2SO_4$ and PAn · HCl. However, they are somewhat worse than those of PAn · CS, which is likely due to lesser planarity and looser packing of the polymer chains in PAn · AMPS. This substance is also a disordered metal characterized by the critical mode of the metal—insulator transition. The Pauli contribution to the paramagnetic susceptibility, as well as the crystallinity of PAn · AMPS increases as the oxidation level increases to attain the optimum value ($y = 0.60$). This suggests that PC of the $R_2$ type, stabilized in the crystalline domains of the specimen, participate in the electron transfer. Quasimetallic clusters in the polymer consist of strongly interacting polymer chains with 3D-delocalized charge carriers.

## Conclusion

The data presented demonstrate a diversity of electronic processes occurring in PAn, which are determined by the structure, conformation, packing, and ordering of the polymer chains, as well as by the structure of the dopant anion introduced into the polymer.

As in other COP, there are both spin and spinless charge carriers (nonlinear excitations, polarons, and bipolarons) in PAn. The ratio of the concentrations of these quasiparticles depends on the properties of the polymer and the anion. A fraction of polarons can collapse into diamagnetic bipolarons on oxidation of PAn. However, this process can be hampered by structural-conformational peculiarities of PAn. The mechanism of charge transport changes on oxidation. The conductivity of a neutral and weakly oxidized PAn is determined by the dynamics of short polarons and/or by isoenergetic charge transfer between polarons and bipolarons. These processes are characterized by a rather strong spin-phonon interaction and determine the anisotropy of the spin dynamics. Since PAn *a priori* has a lower dimensionality than the classical semiconductors, metals, and organic molecular crystals, the anisotropy of the charge transport in such a system is much higher. Oxidation of PAn results in the formation of metal-like clusters of strongly interacting polymer chains with 3D-delocalized charge carriers. A combination of 3D interchain and 1D intercluster VRH charge transport dominates in fully oxidized polymer; each of the mechanisms being characterized by different electron-phonon interactions. The analysis of the magnetic resonance parameters as well as the *ac* and *dc* conductivities showed that metal-like electronic properties become stronger in the order PAn · $H_2SO_4$ → PAn · HCl → PAn · AMPS → PAn · CS.

The data presented in this review show that the spectral resolution achieved in millimeter wave band EPR spectroscopy makes it possible to record more fully and correctly individual spectral lines of organic free radicals with similar structures and different orientations in the external magnetic field. This also permits separate acquisition of a complete set of the magnetic resonance parameters of the PC present in the system. The interaction between the spin packets weakens appreciably in strong magnetic fields. This allows the use of the steady-state SHF saturation and SHF saturation transfer methods as well as the spin label method for obtaining new information on the molecular and electronic processes occurring in PAn and other COP. 2-mm Wave band EPR spectroscopy makes it possible to exploit the potentialities of studying anisotropic spin motions and ultraslow molecular motions in low-dimensional organic semiconductors to the fullest practicable extent. The increase in the recording frequency also increases the sensitivity of the method toward the spin dynamics in highly conducting compounds. High spectral resolution of the method provides a unique possibility of observing fine peculiarities of structural and conformational transitions and electronic processes occurring in PAn and other COP and of interpreting them in the framework of the known approaches.

This work was carried out with financial support of the Russian Foundation for Basic Research (Project No. 97-03-33707).

## References


1. K. Tanigaki, in *Handbook of Organic Conductive Molecules and Polymers*, Vol. 1, Ed. H. S. Nalwa, J. Wiley, Chichester, 1997, 293.
2. J. M. Williams, J. R. Ferraro, R. J. Thorn, K. D. Carlson, U. Geiser, H. H. Wang, A. M. Kini, and M.-H. Whangbo, *Organic Superconductors (Including Fullerenes): Synthesis, Structure, Properties, and Theory*, Prentice-Hall, Englewood Cliffs, New Jersey, 1992.
3. P. Day, in *Handbook of Conducting Polymers*, Vol. 1, Ed. T. E. Scotheim, Marcel Dekker, New York, 1986, 117.
4. G. E. Wnek, in *Handbook of Conducting Polymers*, Vol. 1, Ed. T. E. Scotheim, Marcel Dekker, New York, 1986, 205.
5. *Phtalocyanines: Properties and Applications*, Vol. 4, Eds. C. C. Leznoff and A. B. P. Lever, VCH, Weinheim, 1996.
6. *Conducting Polymers*, Eds. J. L. Brédas and R. Silbey, Kluwer Academic, Dordrecht, 1991.
7. *Conducting Polymers*, Vol. 102, Ed. H. Kiess, Springer-Verlag, Berlin, 1992.
8. *Organic Conductors, Fundamentals and Applications*, Ed. J. P. Farges, Marcel Dekker, New York, 1994.
9. *Electrical, Optical and Magnetic Properties of Organic Solid State Materials*, Vol. 328, Eds. A. F. Garito, A. K.-Y. Jen, C. Y.-C. Lee, and L. R. Dalton, Materials Research Society Symposium Proceedings, Materials Research Society, Pittsburgh, 1994.
10. S. Roth, *One-Dimensional Metals — Physics and Materials Science*, VCH, Weinheim, 1995.
11. *Encyclopedia of Polymeric Materials*, Ed. J. C. Salamone, CRC Press, Boca Raton, 1996.
12. *Handbook of Organic Conductive Molecules and Polymers*, Vols. 1—4, Ed. H. S. Nalwa, J. Wiley, Chichester, 1997.
13. *Conducting Polymeric Materials: Opportunities in Electronics, Optoelectronics, and Molecular Electronics*, Eds. J. L. Brédas and R. R. Chance, NATO Advanced Study Series, Kluwer Academic Publishers, Dordrecht, 1990.
14. *Science and Applications of Conducting Polymers*, Eds. W. R. Salaneck, D. T. Clark, and E. J. Samuelsen, Adam Hilger, New York, 1991.
15. *Molecular Electronics*, Ed. G. J. Ashwell, J. Wiley, New York, 1992.
16. *Application of Electroactive Polymers*, Ed. B. Scrosati, Chapman and Hall, London, 1993.
17. *Organic Conductors: Fundamentals and Applications*, Ed. J.-P. Farges, Marcel Dekker, New York, 1994.
18. *Special Polymers for Electronic and Photonic Applications*, Eds. J. A. Chilton and M. T. Gosey, Chapman and Hall, London, 1995.
19. *Nonlinear Optics of Organic Molecules and Polymers*, Eds. H. S. Nalwa and S. Miyata, CRC Press, Boca Raton, 1997.
20. G. S. Blakemore, *Solid State Physics*, Cambridge Univ. Press, Cambridge, 1985.
21. W. P. Su, J. R. Schrieffer, and A. J. Heeger, *Phys. Rev. B, Condens. Mater.*, 1980, **22**, 2099.
22. R. R. Chance, D. S. Boudreaux, J. L. Brédas, and R. Silbey, in *Handbook of Conducting Polymers*, Vol. 2, Ed. T. E. Scotheim, Marcel Dekker, New York, 1986, 825.
23. R. E. Peierls, *Quantum Theory of Solids*, Oxford University Press, London, 1955.
24. J. C. W. Chien, *Polyacetylene: Chemistry, Physics and Materials Science*, Academic Press, Orlando, 1984.
25. S. Kivelson, *Phys. Rev. Lett.*, 1981, **46**, 1344; S. Kivelson, *Phys. Rev. B, Condens. Mater.*, 1982, **25**, 3798.
26. A. J. Epstein, in *Handbook of Conducting Polymers*, Vol. 2, Ed. T. E. Scotheim, Marcel Dekker, New York, 1986, 1041.
27. H. Stubb, E. Pinkka, and J. Paloheimo, *Materials Science and Engineering*, 1993, **10**, 85.
28. P. Sheng, *Phys. Rev. B, Condens. Mater.*, 1980, **21**, 2180; P. Sheng and J. Klafter, *Phys. Rev. B, Condens. Mater.*, 1983, **27**, 2583.
29. N. F. Mott and E. A. Davis, *Electronic Processes in Non-Crystalline Materials*, Clarendon Press, Oxford, 1979.
30. H. Naarmann, in *Electronic Properties of Conjugated Polymers*, Vol. 76, *Springer Series in Solid State Sciences*, Eds. H. Kuzmany, M. Mehring, and S. Roth, Springer-Verlag, Berlin, 1987, 12.
31. W. Pukacki, R. Zuzok, and S. Roth, in *Electronic Properties of Polymers*, Eds. H. Kuzmany, M. Mehring, and S. Roth, Springer-Verlag, Berlin, 1992, 12.
32. S. Kivelson and A. J. Heeger, *Synth. Met.*, 1988, **22**, 371.
33. M. Peo, S. Roth, K. Dransfeld, B. Tieke, J. Hocker, H. Gross, A. Grupp, and H. Sixl, *Solid State Commun.*, 1980, **35**, 119; L. W. Shacklette, R. R. Chance, D. M. Ivory, G. G. Miller, and R. H. Baughman, *Synth. Met.*, 1980, **1**, 307.
34. A. A. Syed and M. K. Dinesan, *Talanta*, 1991, **38**, 815.
35. J. L. Brédas, R. R. Chance, and R. Silbey, *Mol. Cryst., Liq. Cryst.*, 1981, **77**, 319.
36. J. L. Brédas, R. R. Chance, and R. Silbey, *Phys. Rev. B, Condens. Mater.*, 1982, **26**, 5843.
37. S. Kivelson, *Mol. Cryst., Liq. Cryst.*, 1981, **77**, 65.
38. P. Kuivalainen, H. Stubb, H. Isotalo, P. Yli-Lahti, and C. Holmström, *Phys. Rev. B, Condens. Mater.*, 1985, **31**, 7900.
39. Z. H. Wang, H. H. S. Javadi, A. Ray, A. G. MacDiarmid, and A. J. Epstein, *Phys. Rev. B, Condens. Mater.*, 1990, **42**, 5411.
40. Z. H. Wang, A. Ray, A. G. MacDiarmid, and A. J. Epstein, *Phys. Rev. B, Condens. Mater.*, 1991, **43**, 4373.
41. Z. H. Wang, C. Li, E. M. Scherr, A. G. MacDiarmid, and A. J. Epstein, *Phys. Rev. Lett.*, 1991, **66**, 1745.
42. Z. H. Wang, E. M. Scherr, A. G. MacDiarmid, and A. J. Epstein, *Phys. Rev. B, Condens. Mater.*, 1992, **45**, 4190.
43. E. Punnka, J. Laakso, H. Stubb, and P. Kuivalainen, *Phys. Rev. B, Condens. Mater.*, 1990, **41**, 5914.
44. K. Sato, M. Yamaura, T. Hagiwara, K. Murata, and M. Tokumoto, *Synth. Met.*, 1991, **40**, 35.
45. M. E. Jozefowicz, R. Laversanne, H. H. S. Javadi, A. J. Epstein, J. P. Pouget, X. Tang, and A. G. MacDiarmid, *Phys. Rev. B, Condens. Mater.*, 1989, **39**, 12958.
46. J. M. Ginder, A. F. Richter, A. G. MacDiarmid, and A. J. Epstein, *Solid State Commun.*, 1987, **63**, 97.
47. A. J. Epstein and A. G. MacDiarmid, *J. Molec. Electr.*, 1988, **4**, 161.
48. J. P. Pouget, M. Laridjani, M. E. Jozefowicz, A. J. Epstein, E. M. Scherr, and A. G. MacDiarmid, *Synth. Met.*, 1992, **51**, 95.
49. J. P. Pouget, M. E. Jozefowicz, A. J. Epstein, X. Tang, and A. G. MacDiarmid, *Macromolecules*, 1991, **24**, 779.
50. K. Lee, A. J. Heeger, and Y. Cao, *Synth. Met.*, 1995, **72**, 25.

51. K. Lee and A. J. Heeger, *Synth. Met.*, 1997, **84**, 715.
52. A. J. Epstein, A. G. MacDiarmid, and J. P. Pouget, *Phys. Rev. Lett.*, 1990, **65**, 664.
53. S. Stafström, J. L. Brédas, A. J. Epstein, H. S. Woo, D. B. Tanner, W. S. Huoang, and A. G. MacDiarmid, *Phys. Rev. Lett.*, 1987, **59**, 1464.
54. J. Joo, Y. C. Chung, H. G. Song, J. S. Baeck, W. P. Lee, A. J. Epstein, A. G. MacDiarmid, S. K. Jeong, and E. J. Oh, *Synth. Met.*, 1997, **84**, 739.
55. M. Reghu, Y. Cao, D. Moses, and A. J. Heeger, *Synth. Met.*, 1993, **57**, 5020.
56. A. P. Monkman and P. N. Adams, *Synth. Met.*, 1991, **41–43**, 627.
57. P. N. Adams, P. J. Laughlin, A. P. Monkman, and N. Bernhoeft, *Solid State Commun.*, 1994, **91**, 875.
58. D. C. Trivedi, in *Handbook of Organic Conductive Molecules and Polymers*, Vol. 2, Ed. H. S. Nalwa, J. Wiley, Chichester, 1997, 505.
59. R. P. McCall, J. M. Ginder, M. G. Roe, G. E. Asturias, E. M. Scherr, A. G. MacDiarmid, and A. J. Epstein, *Phys. Rev. B, Condens. Mater.*, 1989, **39**, 10174.
60. F. Zuo, M. Angelopoulos, A. G. MacDiarmid, and A. J. Epstein, *Phys. Rev. B, Condens. Mater.*, 1987, **36**, 3475.
61. A. G. MacDiarmid and A. J. Epstein, *Faraday Discuss. Chem. Soc.*, 1989, **88**, 317.
62. J. Joo, E. J. Oh, G. Min, A. G. MacDiarmid, and A. J. Epstein, *Synth. Met.*, 1995, **69**, 251.
63. M. Nechtschein, in *Handbook of Conducting Polymers*, Eds, T. A. Scotheim, R. L. Elsenbaumer, and J. R. Reynolds, Marcel Dekker, New York, 1997, 141.
64. P. Bernier, in *Handbook of Conducting Polymers*, Vol. 2, Ed. T. E. Scotheim, Marcel Dekker, New York, 1986, 1099.
65. K. Mizoguchi and S. Kuroda, in *Handbook of Organic Conductive Molecules and Polymers*, Vol. 3, Ed. H. S. Nalwa, J. Wiley, Chichester, 1997, 251.
66. K. Mizoguchi, M. Nechtschein, J. P. Travers, and C. Menardo, *Phys. Rev. Lett.*, 1989, **63**, 66.
67. K. Mizoguchi and K. Kume, *Solid State Commun.*, 1994, **89**, 971.
68. K. Mizoguchi and K. Kume, *Synth. Met.*, 1995, **69**, 241.
69. K. Mizoguchi, M. Nechtschein, J. P. Travers, and C. Menardo, *Synth. Met.*, 1989, **29**, E417.
70. K. Mizoguchi, M. Nechtschein, and J. P. Travers, *Synth. Met.*, 1991, **41**, 113.
71. K. M. Salikhov, A. G. Semenov, and Yu. D. Tsvetkov, *Elektronnoe spinovoe ekho i ego primenenie* [*Electron Spin Echo and Its Applications*], Nauka, Novosibirsk, 1976 (in Russian).
72. S. Geschwind, in *Electron Paramagnetic Resonance*, Ed. S. Geschwind, Plenum Press, New York, 1972, 353.
73. Ch. P. Poole, *Electron Spin Resonance*, International Science Publication, London, 1967.
74. L. Kevan and L. D. Kispert, *Electron Spin Double Resonance Spectroscopy*, J. Wiley, New York, 1976.
75. J. S. Hyde and L. R. Dalton, in *Spin Labeling: Theory and Application*, Vol. 2, Ed. L. Berliner, Academic Press, New York, 1979, 1.
76. W. Karte and E. Wehrsdorfer, *J. Magn. Reson.*, 1979, **33**, 107.
77. *Proceedings of the 29th AMPERE — 13th ISMAR Int. Conf. "Magnetic Resonance and Related Phenomena,"* Berlin, 1998, Vols. 1, 2.
78. O. Ya. Grinberg, A. A. Dubinskii, and Ya. S. Lebedev, *Usp. Khim.*, 1983, **52**, 1490 [*Russ. Chem. Rev.*, 1983, **52** (Engl. Transl.)].
79. V. I. Krinichnyi, *2-mm Wave Band EPR Spectroscopy of Condensed Systems*, CRC Press, Boca Raton, 1995.
80. V. I. Krinichnyi, *Appl. Magn. Reson.*, 1991, **2**, 29; V. I. Krinichnyi, *J. Biochem. Biophys. Meth.*, 1991, **23**, 1.
81. V. I. Krinichnyi, *Usp. Khim.*, 1996, **65**, 84 [*Russ. Chem. Rev.*, 1996, **65**, 81 (Engl. Transl.)].
82. V. I. Krinichnyi, *Usp. Khim.*, 1996, **65**, 564 [*Russ. Chem. Rev.*, 1996, **65**, 521 (Engl. Transl.)].
83. V. I. Krinichnyi, *Fiz. Tverd. Tela*, 1997, **39**, 3 [*Sov. Phys.-Sol. St.*, 1997, **39** (Engl. Transl.)].
84. B. Z. Lubentsov, O. N. Timofeeva, S. V. Saratovskikh, V. I. Krinichnyi, A. E. Pelekh, V. I. Dmitrenko, and M. L. Khidekel, *Synth. Met.*, 1992, **47**, 187.
85. F. Lux, G. Hinrichsen, V. I. Krinichnyi, I. B. Nazarova, S. D. Chemerisov, and M.-M. Pohl, *Synth. Met.*, 1993, **53**, 347.
86. V. I. Krinichnyi, S. D. Chemerisov, and Ya. S. Lebedev, *Phys. Rev. B, Condens. Mater.*, 1997, **55**, 16233.
87. V. I. Krinichnyi, S. D. Chemerisov, and Ya. S. Lebedev, *Synth. Met.*, 1997, **84**, 819.
88. V. I. Krinichnyi, S. D. Chemerisov, and Ya. S. Lebedev, *Vysokomol. Soedin., Ser. A*, 1998, **40**, 1324 [*Polymer Sci. A*, 1998, **40**, 826 (Engl. Transl.)].
89. V. I. Krinichnyi, I. B. Nazarova, L. M. Gol'denberg, and H.-K. Roth, *Vysokomol. Soedin., Ser. A*, 1998, **40**, 1334 [*Polymer Sci. A*, 1998, **40**, 835 (Engl. Transl.)].
90. V. I. Krinichnyi, I. B. Nazarova, S. D. Chemerisov, H.-K. Roth, K. Lüders, and G. Hinrichsen, *Synth. Met.*, 1999, in press.
91. V. I. Krinichnyi, A. L. Kon'kin, P. Devasagayam, and A. P. Monkman, *Phys. Rev. B, Condens. Mater.*, 1999, in press.
92. F. A. Neugebauer and P. H. H. Fischer, *Chem. Ber.*, 1965, **98**, 844.
93. F. A. Neugebauer and S. Bamberger, *Angew. Chem.*, 1971, **83**, 47.
94. A. L. Buchachenko and A. M. Vasserman, *Stabil'nye radikaly* [*Stable Radicals*], Khimiya, Moscow, 1973 (in Russian).
95. C. P. Pool, *Electron Spin Resonance. A Comprehensive Treatise on Experimental Techniques*, J. Wiley, New York, 1983.
96. Z. Wilamovski, B. Oczkiewicz, P. Kacman, and J. Blinowski, *Phys. Stat. Sol. B*, 1986, **134**, 303.
97. J. M. Williams, J. R. Ferraro, R. J. Thorn, K. D. Carlson, U. Geiser, H. H. Wang, A. M. Kini, and M.-H. Whangboo, *Organic Superconductors (Including Fullerenes): Synthesis, Structure, Properties, and Theory*, Prentice-Hall, Englewood Cliffs, New Jersey, 1992, Ch. 5, 180.
98. I. B. Goldberg, H. R. Crowe, P. R. Newman, A. J. Heeger, and A. G. MacDiarmid, *J. Chem. Phys.*, 1979, **70**, 1132.
99. R. L. Elsenbaumer, P. Delannoy, G. G. Muller, C. E. Forbes, N. S. Murthy, H. Eckhardt, and R. H. Baughman, *Synth. Met.*, 1985, **11**, 251.
100. R. Cosmo, E. Dormann, B. Gotschy, H. Naarmann, and H. Winter, *Synth. Met.*, 1991, **41**, 369.
101. D. Billand, F. X. Henry, and P. Willmann, *Synth. Met.*, 1995, **69**, 9.
102. I. G. Zamaleev, A. R. Kessel', G. B. Teitel'baum, and E. G. Kharakhash'yan, *Fizika metallov i metallovedenie* [*Metal Physics and Physical Metallurgy*], 1972, **34**, 16 (in Russian).
103. R. Gleiter, W. Schöfer, and M. Eckert-Marsic, *Chem. Ber.*, 1981, **114**, 2309.
104. S. M. Long, K. R. Cromack, A. J. Epstein, Y. Sun, and A. G. MacDiarmid, *Synth. Met.*, 1994, **62**, 287.
105. A. G. MacDiarmid, J.-C. Chiang, A. F. Richter, and A. J. Epstein, *Synth. Met.*, 1987, **18**, 285.

106. V. F. Traven', *Elektronnaya struktura i svoistva organicheskikh molekul* [*Electronic Structure and Properties of Organic Molecules*], Khimiya, Moscow, 1989 (in Russian).
107. J. G. Masters, J. M. Ginder, A. G. MacDiarmid, and A. J. Epstein, *J. Chem. Phys.*, 1992, **96**, 4768.
108. S. A. Al'tshuler and B. M. Kozyrev, *Elektronnyi paramagnitnyi rezonans soedinenii elementov promezhutochnykh grupp* [*Electron Paramagnetic Resonance of Transition-Group Element Compounds*], Nauka, Moscow, 1972 (in Russian).
109. P. R. Gullis, *J. Magn. Reson.*, 1976, **21**, 397.
110. A. E. Pelekh, V. I. Krinichnyi, A. Yu. Brezgunov, L. I. Tkachenko, and G. I. Kozub, *Vysokomol. Soedin., Ser. A*, 1991, **33**, 1731 [*Polymer Sci. USSR, Ser. A*, 1991, **33** (Engl. Transl.)].
111. S. P. Kurzin, B. G. Tarasov, N. F. Fatkulin, and R. Aseeva, *Vysokomol. Soedin., Ser. A*, 1982, **24**, 117 [*Polymer Sci. USSR, Ser. A*, 1982, **24** (Engl. Transl.)].
112. Dz. Reislend, *Fizika fononov* [*Physics of Phonons*], Mir, Moscow, 1975 (Russ. Transl.).
113. V. I. Krinichnyi, A. E. Pelekh, H.-K. Roth, and K. Lüders, *Appl. Magn. Reson.*, 1993, **4**, 345.
114. H.-K. Roth and V. I. Krinichnyi, *Macromol. Chem., Macromol. Symp.*, 1993, **72** 143.
115. H.-K. Roth, V. I. Krinichnyi, M. Schrödner, and R.-I. Stohn, *Synth. Met.*, 1999, **101**, 832.
116. M. A. Butler, L. R. Walker, and Z. G. Soos, *J. Chem. Phys.*, 1976, **64**, 3592.
117. A. Abragam, *The Principles of Nuclear Magnetism*, Clarendon Press, Oxford, 1961.
118. F. Devreux, F. Genoud, M. Nechtschein, and B. Villeret, in *Electronic Properties of Conjugated Polymers*, Vol. 76, Eds. K. Kuzmany, M. Mehring, and S. Roth, Springer-Verlag, Berlin, 1987, 270.
119. L. Pietronero, *Synth. Met.*, 1983, **8**, 225.
120. T. S. Al'tshuler, O. B. Vinogradova, A. F. Kukovitskii, and E. G. Kharakhash'yan, *Fiz. Tverd. Tela*, 1973, **15**, 3602 [*Sov. Phys.-Sol. St.*, 1973, **15** (Engl. Transl.)].
121. A. Carrington and A. D. McLachlan, *Introduction to Magnetic Resonance with Application to Chemistry and Chemical Physics*, Harper and Row Publishers, New York, 1967.
122. S. M. Long, K. R. Cromack, A. J. Epstein, Y. Sun, and A. G. MacDiarmid, *Synth. Met.*, 1993, **55**, 648.
123. F. Zuo, M. Angelopoulos, A. G. MacDiarmid, and A. J. Epstein, *Phys. Rev. B, Condens. Mater.*, 1989, **39**, 3570.
124. A. R. Long, *Adv. Phys.*, 1982, **31**, 553.
125. J. Patzsch and H. Gruber, in *Electronic Properties of Polymers*, Vol. 107, *Springer Series in Solid State Sciences*, Eds. H. Kuzmany, M. Mehring, and S. Roth, Springer-Verlag, Berlin, 1986, 121.
126. V. I. Krinichnyi, N. N. Denisov, H.-K. Roth, E. Fanghänel, and K. Lüders, *Vysokomol. Soedin., Ser. A*, 1998, **40**, 2029 [*Polymer Sci. A*, 1998, **40**, 1259 (Engl. Transl.)].
127. L. Zuppiroli, S. Paschen, and M. N. Bussac, *Synth. Met.*, 1995, **69**, 621.
128. Y. Cao, S. Li, Z. Xue, and D. Guo, *Synth. Met.*, 1986, **16**, 305.
129. Y. W. Park, C. Park, Y. S. Lee, C. O. Yoon, H. Shirakawa, Y. Suezaki, and K. Akagi, *Solid State Commun.*, 1988, **65**, 147.
130. A. B. Kaiser, *Phys. Rev. B, Condens. Mater.*, 1989, **40**, 2806.
131. Y. Nogami, H. Kaneko, T. Ishiguro, A. Takahashi, J. Tsukamoto, and N. Hosoito, *Solid State Commun.*, 1990, **76**, 583.
132. J. Tsukamoto and A. Takahashi, *Synth. Met.*, 1991, **41**, 7.
133. M. C. Itow, T. Kawahara, N. Kachi, H. Sakamoto, K. Mizoguchi, K. Kume, Y. Sahara, S. Masubuchi, and S. Kazama, *Synth. Met.*, 1997, **84**, 749.
134. K. Ausmundtveit, F. Genoud, E. Houz, and M. Nechtschein, *Synth. Met.*, 1995, **69**, 193.
135. T. N. Khazanovich, *Vysokomol. Soedin.*, 1963, **5**, 112 [*Polymer Sci. USSR*, 1963, **5** (Engl. Transl.)].
136. E. A. Silin'sh, M. V. Kurik, and V. Chupek, *Elektronnye protsessy v organicheskikh molekulyarnykh kristallakh: Yavlenie lokalizatsii i polyarizatsii* [*Electronic Processes in Organic Molecular Crystals: Localization and Polarization Phenomena*], Zinatne, Riga, 1988 (in Russian).
137. T. Schimmel, W. Reiss, J. Gimeiner, G. Denninger, M. Schwoerer, H. Naarmann, and N. Theophilou, *Solid State Commun.*, 1988, **65**, 1311.
138. H. H. Wang, B. A. Vogt, U. Geiser, M. A. Beno, K. D. Carlson, S. Kleinjan, N. Thorup, and J. M. Williams, *Mol. Cryst., Liq. Cryst.*, 1990, **181**, 135.
139. L. Forró, G. Sekretarczyk, M. Krupski, D. Schweitzer, and H. J. Keller, *Phys. Rev. B, Condens. Mater.*, 1987, **35**, 2501.
140. N. S. Sariciftci, A. J. Heeger, and Y. Cao, *Phys. Rev. B, Condens. Mater.*, 1994, **49**, 5988.
141. K. Lee, A. J. Heeger, and Y. Cao, *Phys. Rev. B, Condens. Mater.*, 1993, **48**, 14884.
142. M. Iida, T. Asaji, M. B. Inoue, and M. Inoue, *Synth. Met.*, 1993, **55—57**, 607.
143. F. L. Pratt, J. Blundell, W. Hayes, K. Nagamine, K. Ishida, and A. P. Monkman, *Phys. Rev. Lett.*, 1997, **79**, 2855.
144. A. J. Epstein, J. Joo, R. S. Kohlman, G. Du, and A. G. MacDiarmid, *Synth. Met.*, 1994, **65**, 149.
145. P. N. Adams, P. Devasagayam, S. J. Pomfret, L. Abell, and A. P. Monkman, *J. Phys., Condens. Matter*, 1998, **10**, 8293.


*Received June 4, 1999*